

# **ELECTRIC DISCHARGE ABRASIVE DRILLING OF CEMENTED CARBIDE AND HSS**

*A Thesis Submitted*

*in Partial Fulfillment of*

*the Requirements for*

*the Degree of*

**MASTER OF TECHNOLOGY**

**by**

**VIVEK KUMAR**

to the

**Department Of Mechanical Engineering**

**INDIAN INSTITUTE OF TECHNOLOGY, KANPUR**

**April, 1998**

20 MAY 1998 / ME

~~8661 XW DZ~~

CENTRAL LIBRARY  
KAMPUR

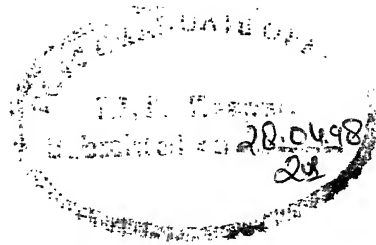
No. A 125485

ME-1998-M-KUM-ELE

Entered in System  
Nimisha  
4.6.98



A125485



## CERTIFICATE

It is certified that the work contained in the thesis titled “ELECTRIC DISCHARGE ABRASIVE DRILLING OF CEMENTED CARBIDE AND HSS ”, by Mr. VIVEK KUMAR, has been carried out under my supervision and it has not been submitted elsewhere for a degree.

  
( Prof. V. K. Jain )

Department of mechanical Engineering  
Indian Institute of Technology  
Kanpur 208016, India

April, 1998

## ACKNOWLEDGMENT

My sincere thanks and regards to the thesis supervisor Dr. V. K. Jain. Without his guidance and constant encouragement, the work would have been almost impossible. A lot of thanks and gratitude to the lab staff (Mr. R. M. Jha, Mr. H.P. Sharma, Mr. Namdev, Mr. Deepak, and others). They assisted to their best while setting up and conducting the experiments. Thanks to Dr. A. P. Verma of HBTI, Kanpur for giving permission and helping in measurement of surface finish. Thanks to the staff of ACMS lab, IIT for helping in SEM analysis of the machined workpieces. At last, I don't want to miss the central workshop people, who did a lot of helping efforts to prepare the workpieces. I must acknowledge the inspiring efforts by Neelesh who immensely helped in planning this thesis.

Life looks dull, if some charm doesn't rush in frequently. My friends (Vikas, Basanti, Bikram, Sambit, Pavan, Khare, Rajani, and others) never did a slack in providing just that, and life was so nice with them!

Last but not the least, the financial support by Department of Science and Technology (DST) is acknowledged.

Vivek Kumar.

## ABSTRACT

Manufacturing needs newer materials for machining of hard materials. This demand is met by the advancement in the material science. Material science has given birth to hard materials which possess high toughness and hardness even at elevated temperatures. These materials possess high value of wear resistance. Due to which they are difficult to machine by abrasion. Non-conventional machining processes such as EDM is widely used in machining of these materials, but low material removal rate is observed. To increase the material removal rate hybrid machining process such as EDDG (electric discharge diamond grinding) is used. In this a metal bonded diamond grinding wheel is used in place of tool electrode in EDM machine. Metal bonded diamond points are used in EDDD (electric discharge diamond drilling), but diamond being too costly forces to think about some alternative abrasive. Diamond is replaced by alumina ( $\text{Al}_2\text{O}_3$ ) abrasives which are much cheaper than diamond. And the process is named as EDAD (electric discharge abrasive drilling). Sparking between the metal bond and work-piece softens the surface of work-piece material. Softened material from work-piece surface is removed by abrasive action. Experiments have been conducted for both cemented carbide and HSS as work-piece materials. Experiments have been conducted for grit sizes of 100/120 and 40/60. A heavy grain pull-out is observed. Bonding material used for manufacturing of alumina drills is copper berrillium which is used for manufacturing of diamond drills. Copper berrillium does not provide good wettability with alumina. Hence, it provides poor bonding strength and results in pull-out of abrasive grains. Pull-out of abrasive grains is more for grit size of 40/60. Penetration rate is more in case of HSS work-piece material. Although, penetration rate obtained during EDAD in all the experiments is lower than that in EDM. This is due to the availability of less area of drill taking part in spark formation during EDAD. Results have been supported by SEM photographs and surface finish measured before and after machining.

# CONTENTS

<b>1 INTRODUCTION</b>	<b>1</b>
1.1 Introduction	1
1.2 Literature survey	2
1.2.1 Abrasive machining of hard materials	2
1.2.2 EDM for hard materials	4
1.2.3 Hybrid machining of hard materials	6
1.3 Scope of the present work	8
1.4 Organization of the thesis	8
<b>2 THEORETICAL ANALYSIS</b>	<b>9</b>
2.1 Metal bonded points	9
2.2 Mechanism of material removal in abrasive machining	10
2.3 Wear mechanism in abasive machining	13
<b>3 EXPERIMENTATION</b>	<b>15</b>
3.1 Experimental set- up	15
3.2 Plan of experiments	19
3.3 Parameters measured	23
<b>4 RESULTS AND DISCUSSIONS</b>	<b>25</b>
4.1 Thrust force	25
4.2 Torque	34
4.3 Penetration rate	36
4.4 Surface finish	39
4.5 SEM analysis	46
<b>5 CONCLUSIONS</b>	<b>52</b>
<b>6 SCOPE FOR FUTURE WORK</b>	<b>54</b>
<b>REFERENCES</b>	
<b>APPENDIX 1</b>	<b>55</b>
<b>APPENDIX 2</b>	<b>56</b>

# **CHAPTER ONE**

## **INTRODUCTION & LITERATURE SURVEY**

### **1.1 INTRODUCTION**

The demand of present industries of machining hard and brittle materials is met by advanced tool materials, which possess high strength even at elevated temperature and also possess excellent wear resistance. These materials are made by 'Powder Metallurgy Technique' in which carbides of refractory materials are arranged in a metal matrix. These materials are widely used in metal cutting industries, die making etc. Due to the lack of appropriate machining methods these materials have not been fully utilized. As these materials have high hardness, conventional machining methods are not suited because the cost incurred in machining may be about 90% of the total cost. Unconventional machining processes are therefore used to machine and shape these materials. There are many unconventional machining processes used for machining hard materials. One of them is EDM which is widely used for machining of cemented carbides due to its ability to produce complex shapes and economical tooling. In EDM, material removal is predominantly by spark erosion; sparking occurs between the tool and work-piece which are connected to opposite polarity and complete the electrical circuit through the dielectric medium. The only constraint of this process is that, both work-piece and tool should be electrically conductive. The minimum conductivity required is 100 ohms-cm. Most of the carbides are non-conductive but they are made conductive so that they can be machined by EDM. ECM is also widely used for machining hard materials, but due to its more power

consumption, costly tooling and less accuracy in comparison to EDM, EDM is preferred. But low MRR (material removal rate) reduces productivity of the EDM.

To increase the material removal rate, EDM is simultaneously done with diamond grinding, the combined process is known as EDDG (electric discharge diamond grinding) and this introduces the hybrid machining process which involves two or more processes simultaneously for machining. Some of the hybrid machining processes used are ECG (electrochemical grinding), plasma hot machining, laser assisted machining, ECAM (electrochemical arc machining), USM (ultrasonic machining ) assisted with EDM etc. In EDDG, metal bonded diamond grinding wheel is used for grinding, sparking occurs between the metal bond and work-piece leading to thermal softening of the work-piece surface. Diamond abrasives at the surface of the rotating diamond wheel remove the softened material from the work-piece surface. Rotary motion of the diamond wheel helps in easy removal of the material. EDDD (electric discharge diamond drilling) is another hybrid process which uses the metal bonded diamond impregnated drills. But diamond is very costly, it increases the cost of machining. To reduce the machining cost, alumina ( $\text{Al}_2\text{O}_3$ ) is used in place of diamond, because alumina is cheaper than diamond and possesses good cutting ability.

## **1.2 LITERATURE SURVEY**

The demand for hard materials is increasing day by day, in the same way demand for the newer machining processes is also increasing to machine these hard materials. The research has been going on since long back and the attempts are being made to develop better methods. These methods can be classified in two categories, the abrasive machining methods and advanced machining methods. However, to take advantage of desirable features of the processes of both these classes, hybrid processes are also being developed. A brief survey of research done in this area is as given below.

### **1.2.1 ABRASIVE MACHINING OF HARD MATERIALS**

Abrasive machining is widely used for the machining of hard materials and most common among the abrasive machining is the grinding process. Hard materials like cemented carbides are generally machined by diamond grinding. The material removal takes place by abrasive action of the abrasives. Carbides possess excellent resistance to abrasion so are difficult to machine even by abrasive action. For machining a material by abrasion, the abrasive should be harder than the work-piece material. Larsen-Basse[1] has suggested that in order that one material can indent and scratch another, it must be at least 20% harder.

Abrasive grains penetrate in the work material as the abrasive grain passes through the grinding zone. Material is initially ploughed aside during grinding at shallow depth of cut followed by chip formation after the grain penetrates to a critical depth. Ploughing action of the grains initiates the cracks in front of the cutting edges of the grains and removes the material from the work surface. In addition to ploughing and chip formation, grinding energy is expended in sliding action between the work piece and the worn area (wear flats) on abrasive grains. The critical rake angle also comes in picture which is the angle at which the tool ceases to form a chip[2]. New grains come in contact with work-piece and some grains get fractured or dislodged from the wheel surface and retained grains get blunted by their repeated contact with the work-piece surface and wear flats. Wear flats on the abrasive grains are considered to be the result of both abrasive action and chemical attack by the work-piece material.

Zelwer and Malkin [3] have examined the grinding mechanism for rock drilling by WC-Co tool bits and revealed that abrasive wear occurs by removal of cobalt metal binder between the WC grains and followed by the carbide removal mainly due to intergranular fracture. Also plastic flow of the WC phase is an important factor in grinding of these materials. Studies have shown that the fracture mechanism of cemented carbide occurs by plastic flow accompanied by crack propagation. Very large residual compressive stresses are developed at the surfaces of WC-Co materials after grinding. These residual stresses are due to plastic deformation at the surface during grinding.

Ritter and Malkin [4] have studied the material removal mechanism for grinding ceramics with diamond wheels and concluded that material removal occurs primarily by

fracture mechanism, some evidences of plastic flow are also found. Modes of fracture observed are transgranular and dislodgment of grains.

Larsen-Basse[5] have investigated the wear mechanism during rotary drilling of abrasive rocks and studied the influence of physical properties on the rate of wear. The main abrasive constituent encountered in the rock is quartz grains which may be classified as soft abrasives with respect to tungsten carbide. Under this condition wear may occur either by the removal of small lumps of composites due to brittle fracture of tungsten carbide skeleton or by the preferential removal of cobalt followed by uprooting and fracture of tungsten carbide grains or by a combination of the two mechanisms.

Moore and King [6] have shown that the fracture mechanism predominates when the depth of indentation of the abrasive is high, the abrasive grains are sharp and ratio of fracture toughness to hardness of the material is low. Using coarse grain abrasives, wear mechanism is explained by fracture and for fine grains it is explained by plastic deformation.

### **1.2.2 EDM FOR HARD MATERIALS**

Many non-conventional machining processes are in use for machining hard materials but most commonly used among them is EDM (electric discharge machining). EDM is used for machining of tool steel, carbide tools and die making. EDM has become popular because of its ability to make complex shaped dies of extremely hard materials in one go, less floor requirements and low tooling cost.

EDM is a process in which the shape of the tool electrode is reproduced on the work-piece. Tool and work-piece both are connected to opposite polarities separately and high frequency sparks are produced between two electrodes. Sparks produces the thermal energy between the tool and work-piece, this thermal energy of sparks is used for material removal. A gap is maintained between the tool and work-piece position to prevent the mechanical contact of two electrodes thus preventing short circuiting.

Pandey and Jilani [7] studied the effects of the pulse parameters and carbide composition on the rate of material removal and relative electrode wear. They experienced the presence of resolidified layer, a large tool wear ratio and thermal cracks. Cobalt influences the machining behavior of carbides. Tungsten carbide having more percentage of cobalt is more likely to show surface cracks and other defects such as pin holes and honeycombs as compared to low percentage cobalt. But cobalt percentage improves the surface finish.

Gadalla and Tsai [8] have used EDM for machining tungsten carbide cobalt composites and found that on increasing the current, frequency of the pulse-on duration to a certain value, the material removal rate is increased. An analysis of the debris showed that in addition to the melting of cobalt matrix, metallic vapours are formed and condense to hollow noncrystalline spheres. These spheres deform and crystallize if crushed. These hollow spheres are made of cooling of cobalt vapours. Also cutting rate increases with the cobalt content and WC grain size because of high electrical conductivity which facilitates in spark formation.

Lenz [9] studied the cracking behavior of sintered carbides during EDM and showed that the cracking pattern is triaxial and follows well defined directions, radial and concentric about the center. Radial cracking starts first, followed by concentric cracking as discharge energy increases. Thermal conductivity of work-piece affects the formation of cracks, poor thermal conductivity produces larger number of cracks. Discharge duration increases the number of cracks and bigger grain size of sintered carbides decreases the number of cracks.

Besides EDM, other processes like ultrasonic machining (USM), electrochemical machining (ECM), abrasive water jet machining, laser machining, electron beam machining have also been used for machining of hard materials. To improve upon the performance of these processes, two processes are combined together and the process is called as 'hybrid process'.

### 1.2.3 HYBRID MACHINING OF HARD MATERIALS

Hybrid machining processes employ two or more processes simultaneously to increase the material removal rate and productivity. Several hybrid machining processes are used, a few of them are as follows.

Electric discharge diamond grinding (EDDG) is a hybrid process which involves EDM with grinding. In this a metal bonded grinding wheel is used to machine the electrically conducting materials. Thermal softening is done by the sparks produced between the wheel and work-piece, and material is removed by grinding wheel due to abrasion. Due to softening of the material, grinding forces and power are reduced in this process. Work-piece itself acts as dressing electrode, so continuous machining is obtained thus increasing material removal rate.

The mechanism of material removal in EDDG has been studied by Philip Koshy, Jain and Lal [10] for cemented carbides. Effects of current and pulse-on time on the material removal rate and grinding forces have been studied. The normal force is measured by varying the current for all the wheel speeds. At each wheel speed, different maxima are obtained and maxima shift towards higher value of current with increasing wheel speed. The reason is that at lower wheel speed, thermal softening is less because of increased discharge instability. Normal force decreases with increase in current for all wheel speeds. The reason is that more thermal softening occurs at higher value of current. The effect of pulse-on time on MRR is that MRR shows a maxima at 0.5 A. The reason for decrease in MRR after a maximum, is the dominance of plastic deformation over microcracking.

The problem of formation of oxide layer in Electrochemical machining is removed in electrochemical grinding (ECG) which involves the combination of ECM and fine grinding of electrically conducting hard materials. Metal bonded grinding wheel is used as cathode and work-piece as anode. Both electrodes are kept immersed in electrolyte. Electrolyte also acts as coolant. About 90% of the material removal takes place due to electrochemical action and rest by abrasion. The oxide layer formed in electrochemical machining is removed by abrasion action by the grinding wheel. As the oxide layer is non-

conducting, so sometimes it stops the process in electrochemical machining which is not in the case of ECG. For materials having hardness higher than  $R_c$  60 or more, ECG gives material removal rates upto ten times of conventional grinding. Better surface finish is obtained in ECG irrespective of hardness, toughness and brittleness of work-piece material. But the dimensional accuracy obtained in ECG is lower than that of conventional grinding. The application of ECG is mainly in manufacturing of carbide tools.

Electrochemical arc machining (ECAM) combines two processes namely ECM and spark erosion. A pulsed voltage is used between the vibrating cathode tool and work-piece anode. A gap is maintained between the tool and work-piece. As the gap decreases, current increases and electrolyte breakdowns and spark is formed. Material removal is by electrolysis. ECAM gives higher material removal rates.

USM (ultrasonic machining ) is combined with EDM to overcome the low material removal rate in the USM. Sparks are generated between the vibrating tool and work-piece which softens the work-piece material and helps in removal of material by abrasive slurry. Vibrating tool forces the abrasives in the slurry to impact on the work-piece material. Abrasive grains easily remove the softened material.

Combined USM and EDM is used in the processing of ceramics[11]. Ultrasonic vibrations are imparted to the grinding wheel. It is reported that grinding forces are reduced by 30%. Grinding of hard materials like TiB has also been studied and, low and constant grinding force have been recorded.

Some hot machining processes have also been used like laser and plasma hot machining. Laser has more power density than plasma. In laser hot machining, work-piece is heated in a particular area and upto certain depth by selecting the parameters, and softened material is removed with the help of tool. Milling of cobalt based alloy has been done successfully by CBN (cubic boron nitride) tool, low cutting forces and higher tool life is reported. Due to low forces it is most successful process in machining of fragile components as the stresses in the work-piece are low and hence safes the work-piece from breaking. Hydrogen and Argon are used as working gases. Plasma hot machining is also successfully used in machining of hard materials eg. ceramics. A plasma jet is used to heat

the work-piece surface. It is reported that the plasma hot machining may change the mode of chip formation from discontinuous (brittle fracture type) to continuous (plastic fracture type) since the ceramic softens and deforms in a plastic manner at high temperature above 800 ° C. Also wear of the tool is decreased in plasma hot machining[12].

### 1.3 SCOPE OF THE PRESENT WORK

The present work in this thesis is based on a hybrid machining process, i.e. electric discharge abrasive drilling (EDAD) using metal bonded points. Diamond, the hardest abrasive material known, has been used earlier as abrasive in the metal bonded points but, the cost of the diamond forces to think about some alternative abrasive. In this work, alumina ( $\text{Al}_2\text{O}_3$ ) has been used in place of the diamond. Experiments have been conducted for cemented carbides and HSS (high speed steel) as work-piece materials to study the effect of pulse-on time on thrust force, torque and material removal rate. By conducting the experiments for cemented carbides and HSS, the effect of work-piece material has also been studied.

### 1.4 ORGANISATION OF THE THESIS

**Chapter one** starts with the introduction and the literature available related to the topic and gives the way in which EDAD process has been approached for machining hard materials.

**Chapter two** includes the mechanism of material removal from work-piece surface. Wear mechanism of metal bonded points is also presented in this chapter. Type of metal bonded points used is also mentioned in this chapter.

**Chapter three** contains plan of experiments, experimental set-up used and procedure of experiments.

**Chapter four** includes the values of thrust force, torque, MRR obtained by experiments and detailed analysis of these parameters. SEM analysis of unmachined and machined surface of work-pieces is also presented in this chapter. Surface roughness values are also mentioned in this chapter.

**Chapter five and six** ends with conclusion and scope for future work.

## **CHAPTER TWO**

### **THEORETICAL ANALYSIS**

The results obtained in the experiments have been analyzed with the help of theories proposed by various researchers. The mechanism of material removal and wear in drilling has also been analyzed to understand the process during abrasive drilling.

#### **2.1 METAL BONDED POINTS**

In electric discharge abrasive machining metal bonded points are used. In this, abrasive grains are uniformly distributed in the metal matrix. Abrasive grains are electrically non-conducting but the metal bond between the abrasive grains is conducting. It makes the drill electrically conducting. Earlier, diamond has been used as abrasive which is available in two types [13] namely.

- 1 Surface set bits.
- 2 Impregnated core bits.

In **SURFACE SET BITS**, a layer of diamond abrasive grains is set on the core of the drill. These diamond grains which are on the surface are used for grinding. These are used for internal cylindrical grinding. Fig. 2.1 shows the cross-sectional view of a surface set bit.

**IMPREGNATED CORE BITS** are made by distributing diamond abrasive grains in the bronze matrix. Thus diamond abrasive grains are uniformly distributed in the bronze

matrix. During machining, diamond abrasive grains at the surface of the bit wear out and new abrasive grains are exposed on the surface of drill. So new abrasive grains continuously exposed in machining and continuous machining is obtained. Fig.2.2 shows the cross-sectional view of an impregnated core bit.

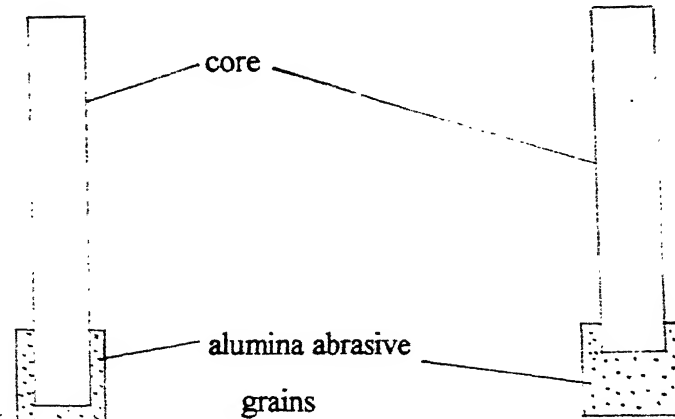


Fig. 2.1 Surface set bit.

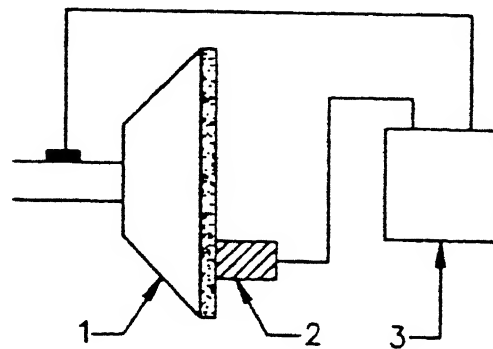
Fig. 2.2 Impregnated core bit.

In the present work, alumina abrasive grains have been used for electric discharge abrasive drilling because diamond is a costly abrasive and alumina abrasives are cheaper than diamond. Surface set bit type alumina abrasive drills were specially manufactured for our purpose by WENDT (INDIA) LTD ,HOSUR. The bonding material used in the manufacturing of these drills is copper-berrillium which is used for manufacturing of diamond drills. So, bonding between the alumina abrasives and bonding material is not so good because of inadequate wetting action between them. As discussed in the 'Results and Discussions' chapter, this has led for easy pull-out of the abrasives from the bonding material.

## 2.2 MECHANISM OF MATERIAL REMOVAL IN ABRASIVE MACHINING

In abrasive machining, tool material should be harder than work-piece. So grinding of hard materials poses a problem for machining as the hardness of the work

material increases. Machining forces also increases as the hardness increases because the indentation of the abrasive grains in the work material becomes difficult. Hence, to reduce the normal force in machining, abrasive machining is accompanied with EDM and the process is known as electric discharge abrasive machining. One such process is EDDG (electric discharge diamond grinding) which uses diamond abrasives. Fig. 2.3 shows the configuration of the EDDG process. In EDDG, metal bonded diamond wheel is used for grinding. Sparking occurs between the metal bond of grinding wheel and the work-piece (conducting). Work-piece material gets softened and diamond wheel removes the material from work-piece surface by abrasion. Material removal in EDDG takes place by melting, vaporization and abrasion.



(1-wheel, 2-work, 3-power supply,

Fig. 2.3 Basic configuration of EDDG process[14].

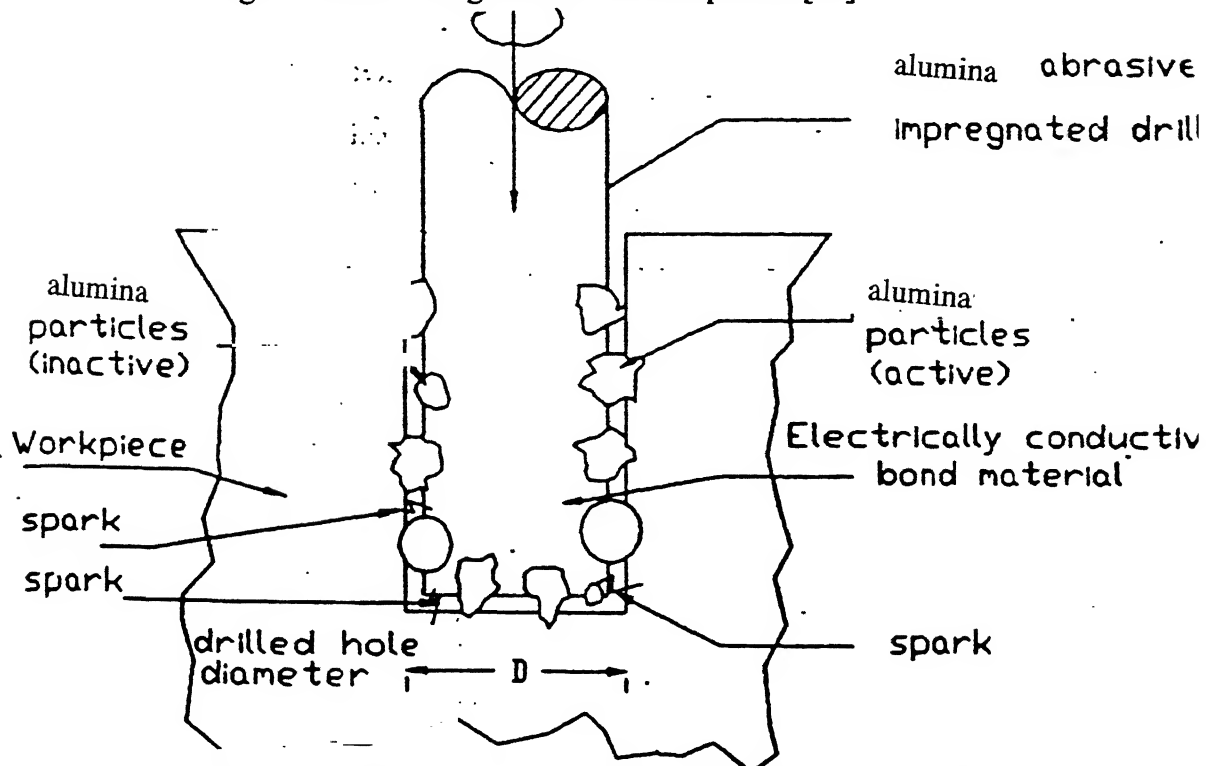


Fig. 2.4 Alumina abrasive grains in contact with work-piece in EDAD[15].

Alumina grains in contact with the work-piece material in EDAD are shown in Fig 2.4 where material removal takes place mainly by two processes.

- 1 Plastic deformation of material.
- 2 Initiating cracks.

Material removal in ductile materials is predominantly due to plastic deformation and in brittle materials by initiating cracks. In plastic deformation, grooves are generated in the work-piece. While in brittle materials, if the depth of indentation is higher than a critical value, tensile stress associated with the sliding initiates the median and lateral cracks in the work-piece material. Material is removed from work-piece surface due to fracture when the cracks reach the free surface of the work-piece or link themselves to form the loose fragments. Wear of coarse abrasives takes place predominantly due to fracture mechanism, while that of fine abrasives due to plastic deformation mechanism. The rate of material removal in case of fracture mechanism is higher than that of plastic deformation, since the volume removed by cracks is large compared to groove dimensions. Since both plastic deformation and fracture mechanism are likely to occur during the abrasive wear of brittle materials so it is necessary to know under what conditions either plastic deformation mechanism or fracture mechanism may predominate and control the rate of material removal.

The material removal mechanism of cemented carbides during indentation has been discussed by Ogilvy [16] . He observed that in cemented carbides, the cracks remain within the plastic zone of indentation unlike in brittle solids, where they penetrate the surrounding elastic strain field. Both plastic deformation and microcracking mechanisms occur in abrasion of cemented carbides so rate of material removal will be governed by the relative extent of these mechanisms. Plastic deformation is favoured when the load on the abrasive grains is small, i.e. for small abrasive grain sizes or low applied loads and when the ratio of fracture toughness to hardness of the material is high and vice versa for fracture mechanism.

## 2.3 WEAR MECHANISM IN ABRASIVE MACHINING

Wear is an important factor during machining, it affects the material removal rate and the force experienced during machining. Therefore, to know about the wear is as important as to know about material removal mechanism. The wear observed for tungsten carbide such as abrasion wear, erosion wear and impact wear are analyzed by microscopic examination of the wear surface. Wear mechanism is mainly classified in following categories[17].

1 Micromachining.

2 Impact.

3 Adhesion.

4 Thermal.

5 Chemical.

In *Micromachining* wear mechanism, abrasive grains act as a cutting tool and remove the work-piece material in the form of chip. In *Impact* wear mechanism, localized and sudden application of high compressive stresses cause crushing of the material. In *Adhesion* wear mechanism, high temperature causes localized welding, followed by tearing near the welds. In *Thermal* wear mechanism, stresses induced by thermal expansion cause fracture. And in *chemical* wear mechanism, reactions occur between the material and chemically active species in the environment.

In general more than one wear mechanism occur at the same time. So it is called abrasive wear to represent the existing mechanism. Fig.2.5 shows the abrasive grains of metal bonded point penetrating in the work material.

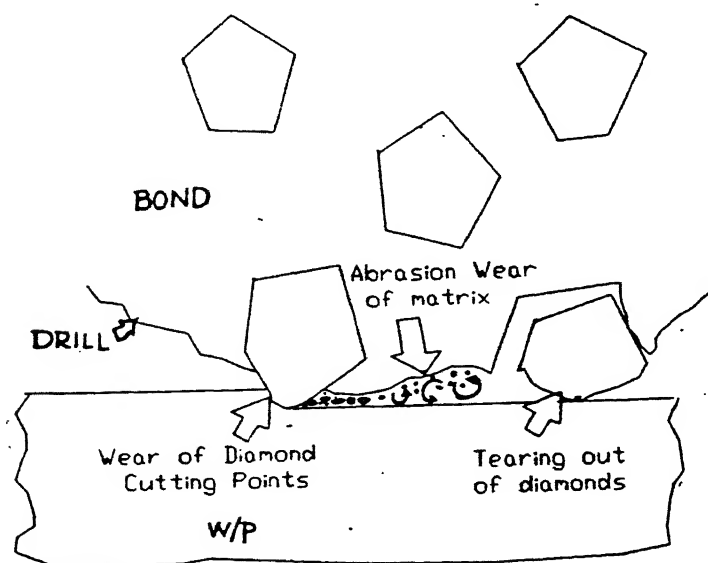


Fig. 2.5 Penetration of diamond grains in work-piece surface[13].

While grinding hard materials, abrasive grains come in contact with the work-piece surface and penetrate in the surface of work-piece and material is removed by abrasive action. As depth of penetration increases, abrasives grains start wearing. Abrasive grains get blunted and wear flats are formed on the abrasive grains. These blunted abrasive grains do not remove material but rub on the surface. This is known as glazing of the wheel. Chips get lodged in the space between the grains and loads the wheel. These two phenomena increase, force and power in machining. Wear of diamond wheel is due to one, or combination of the following phenomena [18].

- ~ Wear of grits resulting in the formation of wear flats.
- ~ Wheel loading.
- ~ Pull-out of abrasive grains.

Although, during machining of cemented carbides fine microfracture of the abrasive grains to a large extent reduces the wear flat formation but, area under the wear flat keeps on increasing and reaches such a size that the force acting on the grains attains some critical magnitude which results in grain fracture or pull-out. Thus a well worn grain is lost from the wheel and it may be considered to be replaced by a sharp grain with a resulting drop in grain force. After a sufficient amount of grinding, abrasive wear, fracture wear and pull-out of the grains occur simultaneously over the entire working surface of the wheel. The total wear flat area attains a steady value and the force component becomes constant. While grinding tool steels by diamond abrasive both abrasive and chemical attacks are reported and chemical effect reduces as the carbon content in the tool steel increases [19].

## **CHAPTER THREE**

### **EXPERIMENTATION**

#### **3.1 EXPERIMENTAL SET-UP**

The following devices are needed to perform the electric discharge drilling (EDD) and electric discharge abrasive drilling (EDAD), and to evaluate the performance.

- ~ Dynamometer.
- ~ Recording device.
- ~ Weight measuring device.
- ~ Electric discharge machine.
- ~ Drilling attachment.

**DYNAMOMETER** is used for measuring the thrust force and torque coming in the process. Dynamometer was designed and fabricated by Ankulkar [] by assuming the spokes of the wheel as fixed beam. Fig 3.1 shows the beam of the dynamometer. Earlier the strain gauges were fixed on the arms using Fevi Quick. It was found that it gave rise to conductivity problem i.e. it lost its non-conducting nature. As a result, in this dynamometer, strain gauges have been fixed by Bakelite adhesive. The procedure for mounting the strain gauges is as follows. First the oxide layer from the ends of the gauges is removed by rubbing them, keeping in mind that very little force should be applied so that they may not break. Then strain gauges are temporarily pasted on the Teflon rod by ordinary gum. A drop of bakelite adhesive is put on the place where the strain gauge is to be fixed. The place is already made nonconducting by sticking a small sheet of Teflon on it

with the help of Fevi Quick. Now the strain gauge pasted on the Teflon rod is fixed on the Teflon sheet by bakelite adhesive. In this way all the gauges are mounted one by one and connections are taken from their ends by soldering. Plastic coated wires are used for taking the connections from the ends of the strain gauges. The plastic coated wires are in the form of strip, so connections are taken out of dynamometer by FRC connector. The connections are made in two wheat-stone bridges separately each for thrust and torque. The two wheat-stone bridges are shown in the Fig. 3.2 (a) and strain gauges are numbered for convenience. Fig. 3.2 (b) shows the configuration of the dynamometer. A constant 6.0 V D.C. supply is used for wheat-stone bridges. The corresponding position of the gauges is also seen in cross-sectional view of the dynamometer. Finally strain gauges are sealed by Araldite.

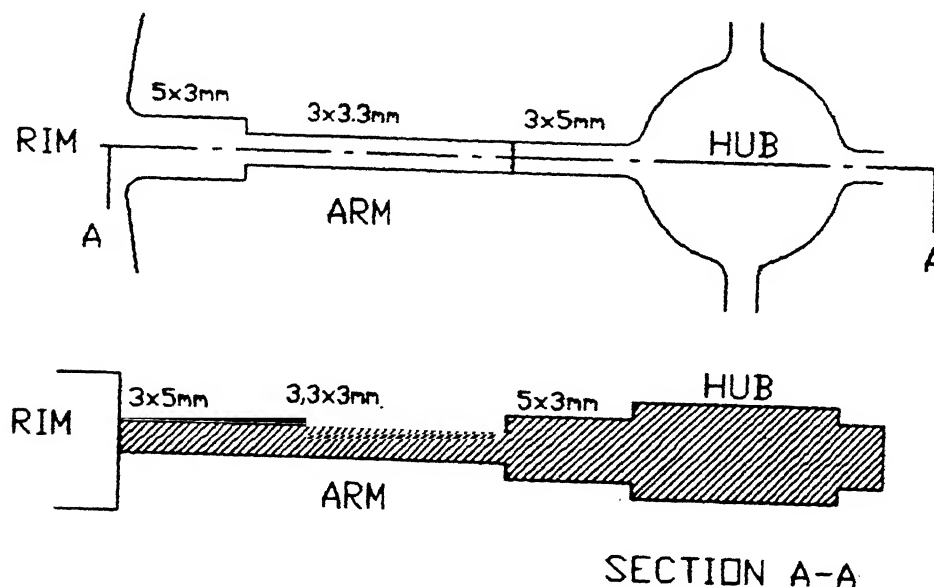
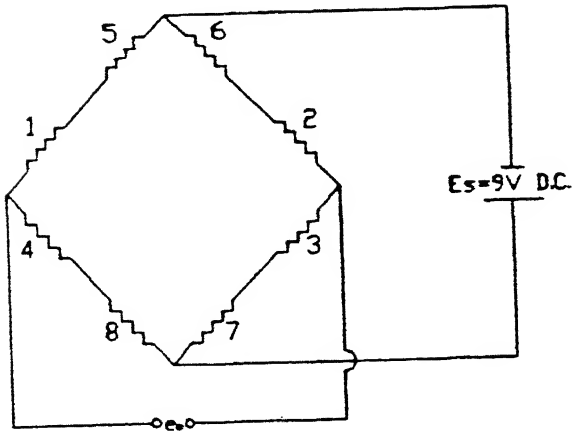


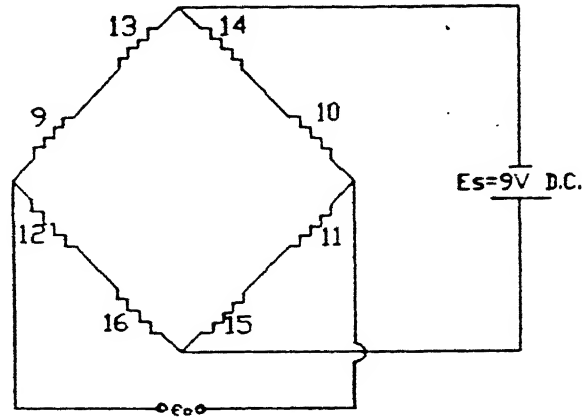
Fig. 3.1 Arm of dynamometer [15].

**RECORDING DEVICE** is used to record the thrust force and torque experienced by the dynamometer. Two separate pens move simultaneously on the moving graph paper to give the thrust force and torque values. Omniscrimer recorder available in the laboratory has been used. A 6.0 V constant D.C. supply is given to the recorder and recorder is balanced by the potentiometer connected between the dynamometer and

recorder. A separate potentiometer is used for thrust force and torque wheat-stone bridges. All the readings have been noted at the minimum voltage of 0.005m V .



Wheatstone bridge for  
thrust measurement



Wheatstone bridge for  
torque measurement

Fig. 3.2 (a) Wheatstone bridges for thrust and torque measurement [15].

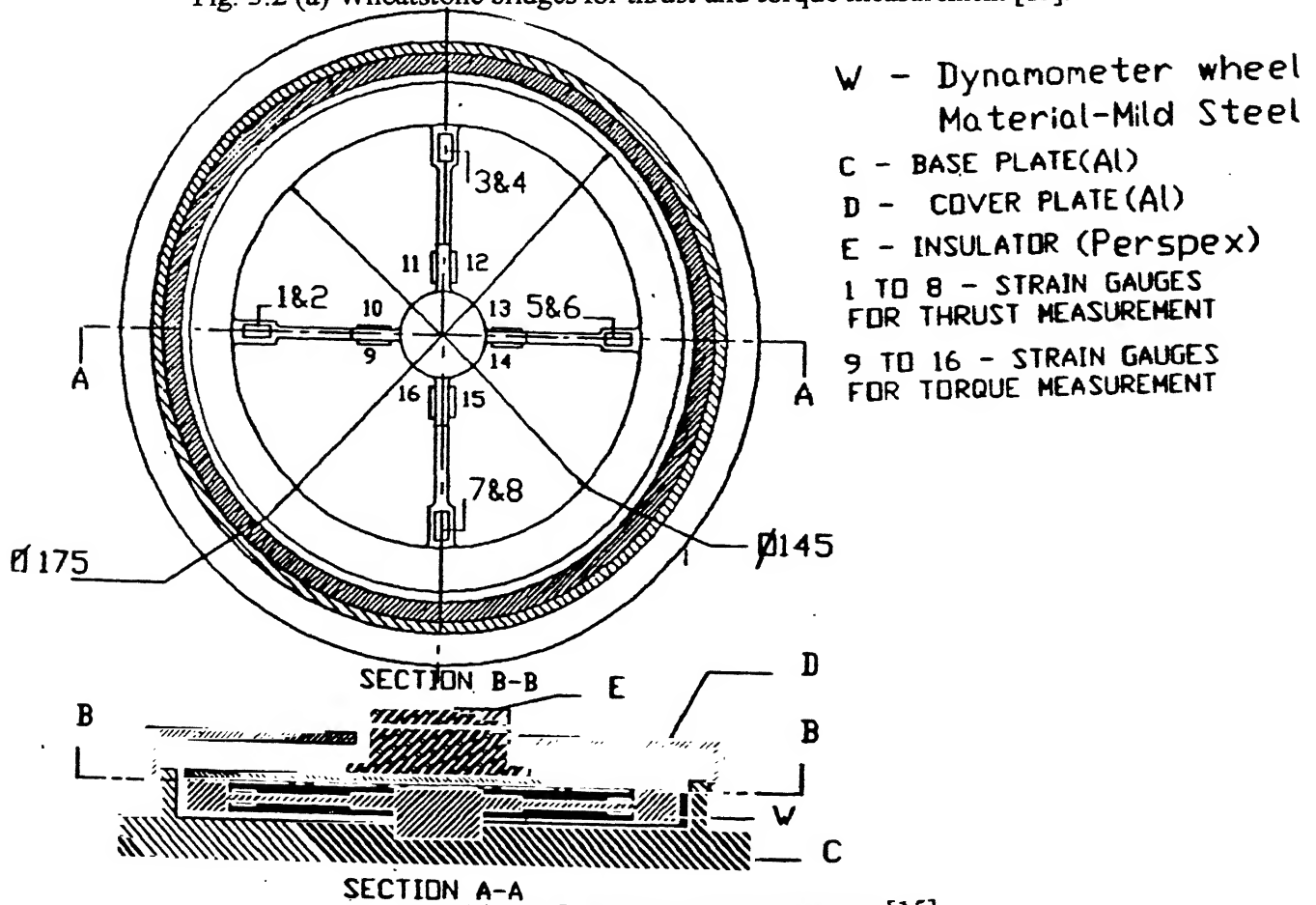


Fig. 3.2 (b) Configuration of dynamometer [15].

**WEIGHT MEASURING DEVICE** used here is Afcoset electronic balance which has a least count of 0.001 g.

**ELECTRIC DISCHARGE MACHINE** used here is **ELEKTRA PULS R35** spark erosion type equipped with a voltage stabilizer and a pump with filter to supply kerosene as dielectric.

**DRILLING ATTACHMENT** is shown in the Fig. 3.3. It has a motor to rotate the drill. Motor is connected to the variac (dimmerstat) for varying the speed. Drilling attachment is made of mild steel (conductive) for providing polarity to the drill. Tachometer is used to measure the speed of the drill and stop watch to note the time during the experiments.

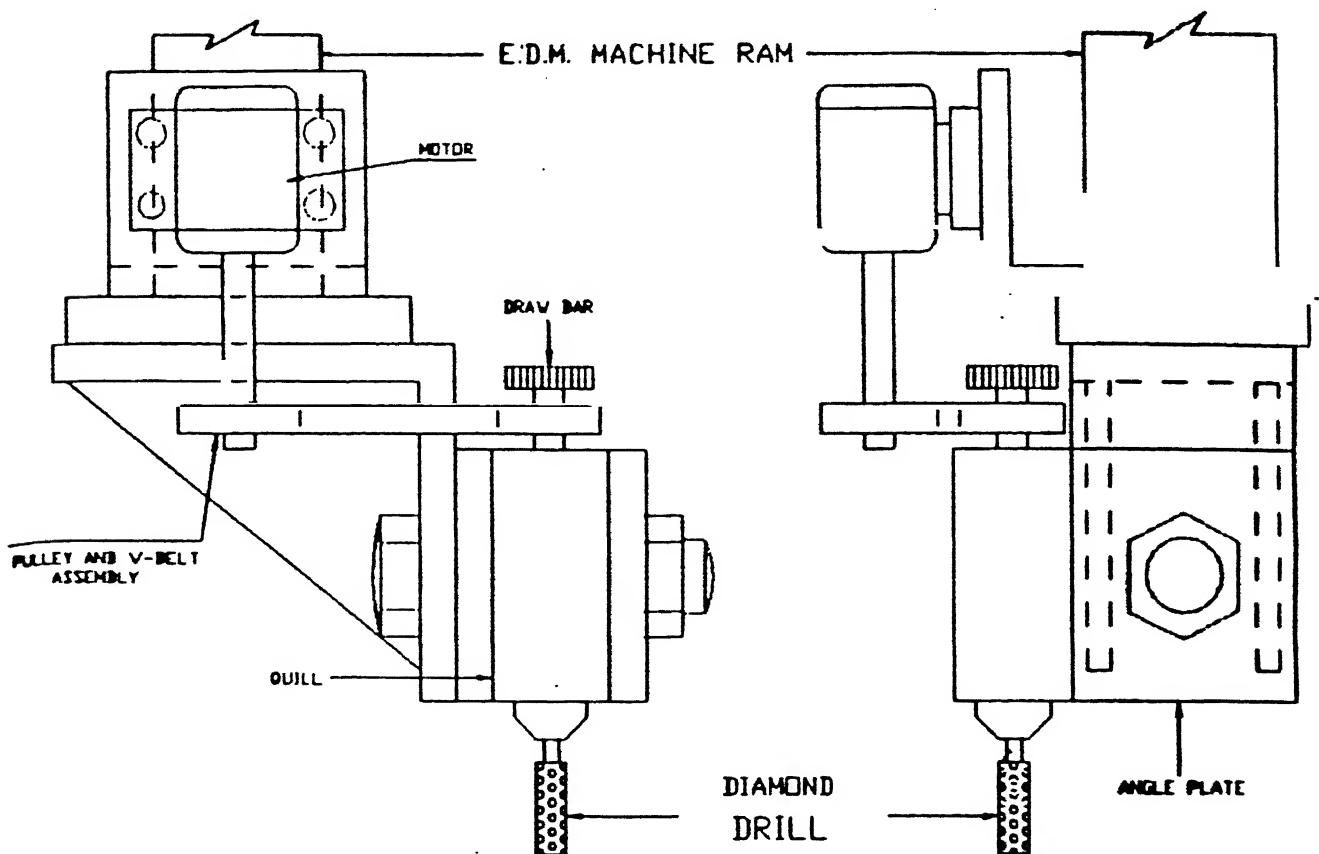


Fig. 3.3 Drilling attachment [15].

### 3.2 PLAN OF EXPERIMENTS

Plan of the experiments is imperative before conducting them. Here the experiments have been planned by keeping some parameters constant and varying a particular parameter whose effect is to be considered. The particular parameter is pulse-on time. In all the experiments, duty factor is kept constant. Duty factor is the ratio of pulse on-time to the pulse duration. Mathematically, it can be expressed as:

$$\tau = \frac{T_{ON}}{\text{Pulse Duration}}$$

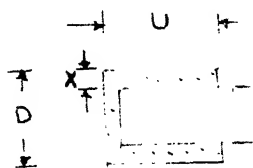
$$\text{Pulse Duration} = T_{ON} + T_{OFF}$$

Koshy [18] has observed that MRR and normal force shows a maxima at 0.5 A. To get a significant value of above parameters, current is fixed at 0.5 A. The experiments conducted on EDAD are compared with the results previously obtained for EDDD (electric discharge diamond drilling). Hence, same parameters as used in EDDD are chosen for EDAD. The plan of experiments which is as follows:

#### SET NO 1

Using the alumina tool of specification 512 - 10 - 8 - 2 - Al - 100/120 100 C .

Following figure shows the dimensions of the alumina drill.



512 - TYPE

10 - D

8 - U

2 - X

Al - Alumina abrasive

100/120 - grit size

100 C - Concentration

all dimensions in mm.

Fig. 3.4 Alumina abrasive drill showing all dimensions.

**FIXED PARAMETERS**

Voltage ,  $V=30$  V

Current ,  $I=0.5$  A

Duty factor ,  $\tau=0.5$

Grit Size of Tool Abrasives 100/120 .

Work-piece material cemented carbide .

Work-piece polarity negative .

EXP. NO.	PULSE ON - TIME ( $\mu$ S)
1 C	2
2 C	5
3 C	10
4 C	20

**SET NO 2**

Using alumina tools having specification as 512 - 10 - 8 - 2 - Al - 100/120 100 C.

**FIXED PARAMETERS**

Voltage ,  $V=30$  V

Current ,  $I=0.5$  A

Duty factor ,  $\tau=0.5$

Grit Size of the Tool Abrasives 100/120 .

Work-piece material HSS (high speed steel) .

Work-piece polarity negative .

EXP.NO.	PULSE ON - TIME ( $\mu$ s)
1 H	2

2 H	5
3 H	10
4 H	20

### **SET NO. 3**

Using alumina tools having specification 512 - 10 - 8 - 2 - Al - 40/60 100 C.

In this drill, grit size of abrasives is 40/60 and dimensions are same as given in Fig. 3.4

#### **FIXED PARAMETERS**

Voltage ,  $V=30$  V

Current ,  $I=0.5$  A

Duty factor ,  $\tau=0.5$

Grit Size of the Tool Abrasives 40/60 .

Work-piece material HSS (high speed steel) .

Work-piece polarity negative .

EXP.NO.	PULSE ON - TIME ( $\mu s$ )
5 H	2
6 H	5
7 H	10
8 H	20

### **SET NO.4**

Using the alumina tool of specification 512 - 10 - 8 - 2 - Al - 40/60 100 C.

#### **FIXED PARAMETERS**

Voltage ,  $V=30$  V

Current ,  $I=0.5$  A

Duty factor ,  $\tau=0.5$

Grit Size of Tool Abrasives 40/60 .

Work-piece material cemented carbide .

Work-piece polarity negative .

EXP. NO.	PULSE ON - TIME ( $\mu$ S)
5 C	2
6 C	5
7 C	10
8 C	20

**SET NO.5**

Using copper tool having same dimensions as abrasive tool .

**FIXED PARAMETERS**

Voltage ,  $V=30$  V

Current ,  $I=0.5$  A

Duty factor ,  $\tau=0.5$

Work-piece material cemented carbide .

Work-piece polarity negative .

EXP. NO.	PULSE ON - TIME ( $\mu$ S)
1 C E	2
2 C E	5
3 C E	10
4 C E	20

**SET NO. 6**

Using copper tool having same dimensions as abrasive tool.

**FIXED PARAMETERS**

Voltage ,  $V=30$  V

Current ,  $I=0.5$  A

Duty factor ,  $\tau=0.5$

Work-piece material HSS (high speed steel) .

Work-piece polarity negative .

EXP.NO.	PULSE ON - TIME ( $\mu s$ )
1 H E	2
2 H E	5
3 H E	10
4 H E	20

### 3.3 PARAMETERS MEASURED

The following parameters have been measured in above experiments.

1. Thrust force.
2. Torque.
3. Penetration rate.
4. Surface finish.

SEM analysis of machined and unmachined surfaces is done by scanning electron microscope. Thrust force and Torque have been measured using the graph obtained from the Recorder. Penetration rate is calculated by the following formula.

$$PR = [MRR \div (DENSITY \times AREA)] \times 10$$

Where MRR is in g/s , density in g/cm<sup>3</sup> , area of the bottom of drill in cm<sup>2</sup> . Penetration rate (PR) in mm/s.

Plan of experiments can be put in a tabular form as:

Table 3.1 Plan of experiments for EDAD.

EXP. NO.	VOL. V (V)	CURR. I (A)	DUTY FACTOR	PULSE ON-TIME ( $\mu s$ )	GRIT SIZE	W/P MATERIAL
----------	---------------	-------------	-------------	---------------------------	-----------	--------------

1 C	30	0.5	0.5	2	100/120	cemented carbide
2 C	30	0.5	0.5	5	100/120	cemented carbide
3 C	30	0.5	0.5	10	100/120	cemented carbide
4 C	30	0.5	0.5	20	100/120	cemented carbide
5 C	30	0.5	0.5	2	40/60	cemented carbide
6 C	30	0.5	0.5	5	40/60	cemented carbide
7 C	30	0.5	0.5	10	40/60	cemented carbide
8 C	30	0.5	0.5	20	40/60	cemented carbide
1 H	30	0.5	0.5	2	100/120	HSS
2 H	30	0.5	0.5	5	100/120	HSS
3 H	30	0.5	0.5	10	100/120	HSS
4 H	30	0.5	0.5	20	100/120	HSS
5 H	30	0.5	0.5	2	40/60	HSS
6 H	30	0.5	0.5	5	40/60	HSS
7 H	30	0.5	0.5	10	40/60	HSS
8 H	30	0.5	0.5	20	40/60	HSS

Table 3.2 Plan of experiments for EDM.

EXP. NO.	VOL. V (V)	CURR. I (A)	DUTY FACTOR	PULSE ON - TIME ( $\mu s$ )	W/P MATERIAL
1C E	30	0.5	0.5	2	cemented carbide
2C E	30	0.5	0.5	5	cemented carbide
3C E	30	0.5	0.5	10	cemented carbide
4C E	30	0.5	0.5	20	cemented carbide
1H E	30	0.5	0.5	2	HSS
2H E	30	0.5	0.5	5	HSS
3H E	30	0.5	0.5	10	HSS
4H E	30	0.5	0.5	20	HSS

## **CHAPTER FOUR**

### **RESULTS AND DISCUSSIONS**

Experiments have been conducted and values of thrust force, torque and penetration rate have been calculated. The trends of variation of these parameters with pulse on-time are plotted and analyzed with the help of mechanism proposed by various researchers. Duty factor is defined as the ratio of pulse-on time and pulse duration. Pulse duration is the sum of  $T_{ON}$  and  $T_{OFF}$ . Mathematically, it can be expressed as:

$$\tau = \frac{T_{ON}}{\text{Pulse Duration}}$$

$$\text{Pulse Duration} = T_{ON} + T_{OFF}$$

Duty factor is kept constant during the experiments at a value of 0.5 . As pulse-on time increases, pulse duration also increases so as to keep the duty factor constant. Hence,  $T_{OFF}$  also increases with increase in  $T_{ON}$ .

#### **4.1 THRUST FORCE**

The time evaluation of thrust force during machining is shown in the graph obtained from the recorder for HSS and cemented carbide in Fig. 4.1 and 4.2. Time evaluation of thrust force gives the on-line behaviour of the thrust force. The thrust force has been measured after every two boxes and average of all the values is calculated to give the 'average thrust force'. Graphs have been plotted for two different grit sizes (100/120 , 40/60) of the abrasives used in the drills, and also for HSS and cemented carbide

separately. The variation of thrust force with pulse-on time in EDAD for HSS is shown in Fig. 4.3. Thrust force increases with the increase in pulse on-time.

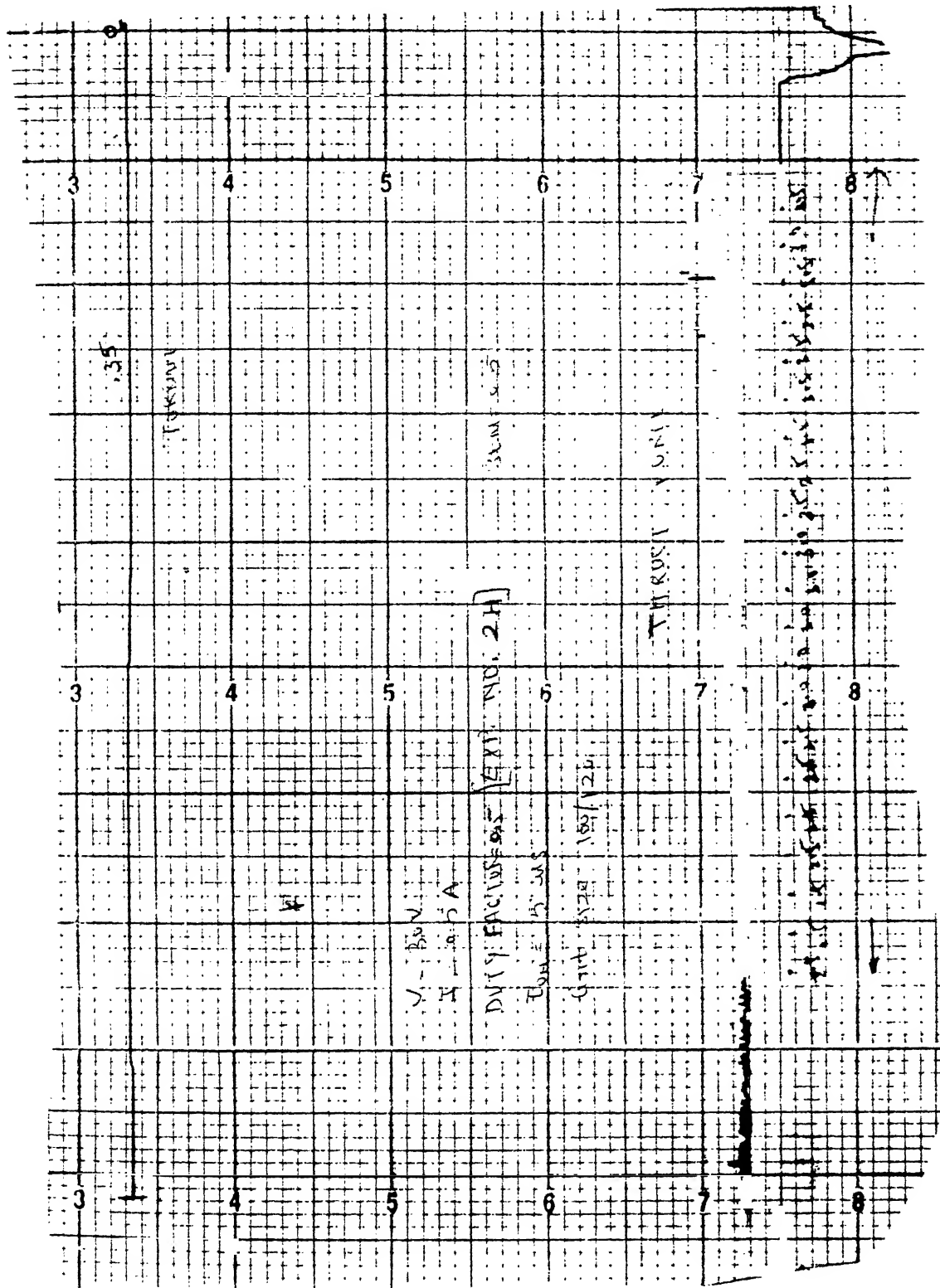


Fig. 4.1 Time evaluation of Thrust Force and Torque during machining HSS.

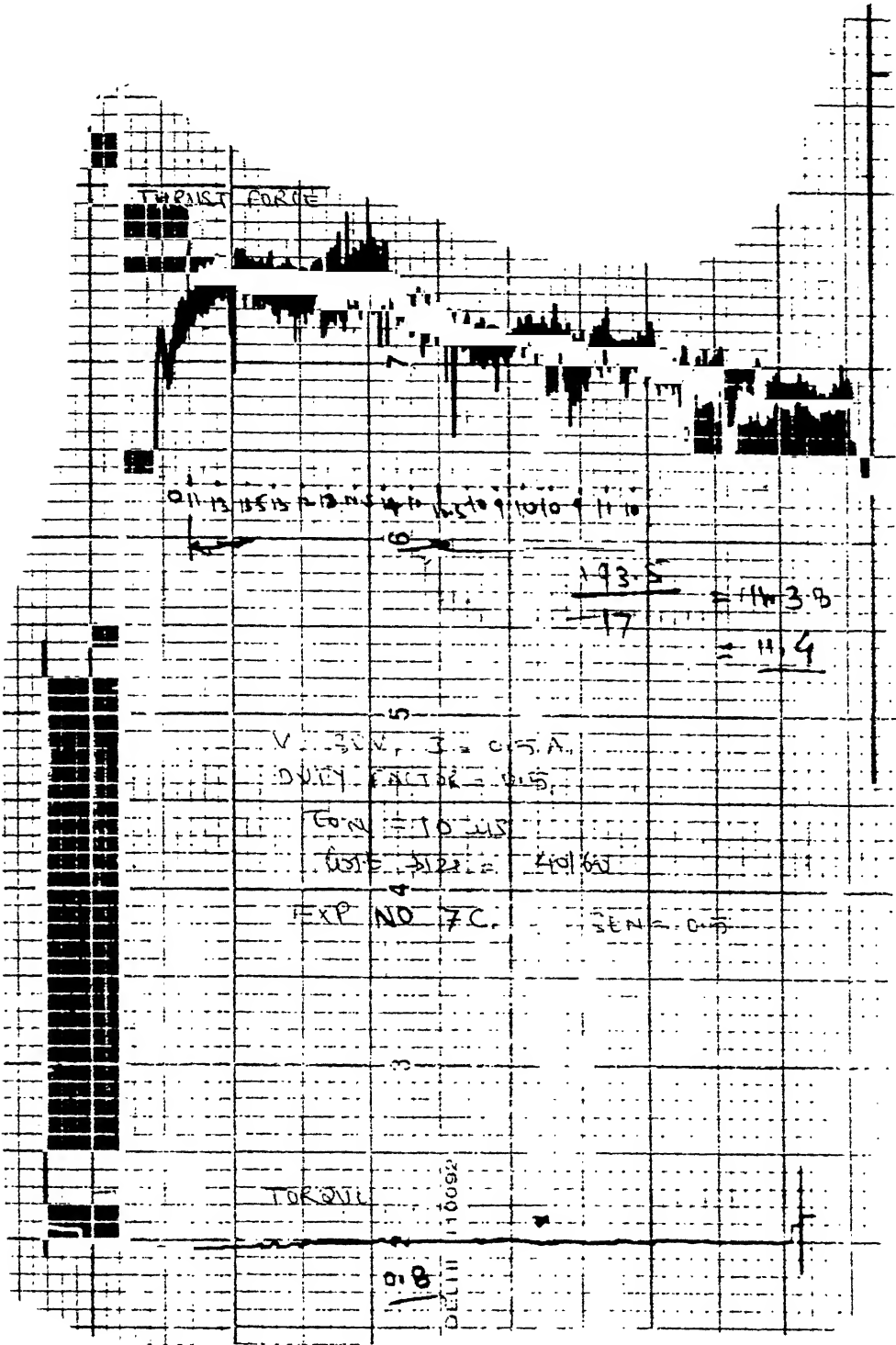


Fig. 4.2 Time evaluation of Thrust Force and Torque during machining cemented carbide.

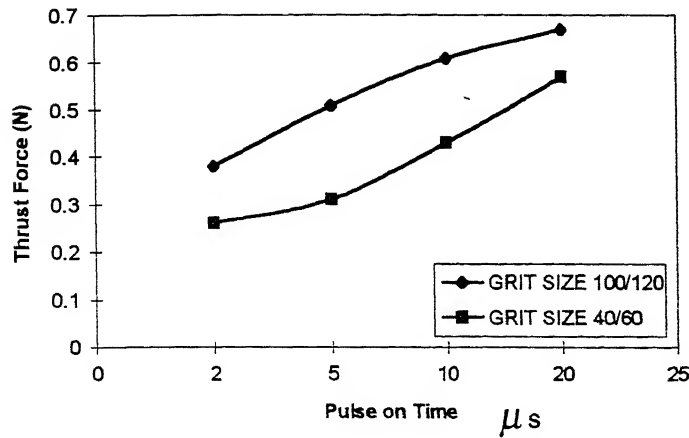


Fig. 4.3 Thrust force variation with pulse-on time in EDAD for HSS.

On increasing the pulse on-time ( $T_{ON}$ ),  $T_{OFF}$  also increases. Therefore, melted material gets more time for heat dissipation in the interior of work-piece. This reduces the thermal softening of the work-piece material[7]. Due to reduced thermal softening of work-piece material, thrust force increases with increase in pulse on-time [10] as shown in Fig. 4.3. Fig. 4.4 shows the behaviour of normalised force Vs time for different values of current for cemented carbide. Line 1 represents the self dressing behaviour. Line 2 for grit blunting phenomena. and line 3 represents the pull-out of abrasives. If thrust force decreases with time before attaining steady state, it indicates pulling-out of the abrasives[20].

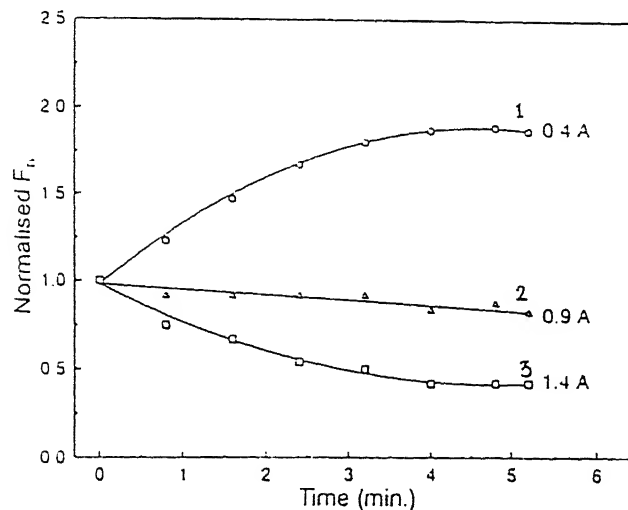


Fig. 4.4 Variation of normalised force with time while grinding cemented carbide[20].

At lower pulse on-time, gap between the work-piece and tool is low, hence depth of penetration is more. Pull-out of abrasive grains is more at more depth of penetration. The bonding material used for bonding abrasives in drills is copper berillium which has been commonly used for bonding diamond grains in metal bonded diamond points. So bonding strength is not so good. The probability of pulling-out of bigger abrasives is more as grains protrude more out of the tool surface. Fig. 4.5 shows the two sizes of the grains protruding out from the tool surface. At lower pulse on-time, depth of penetration is more, so larger grains pull-out in more numbers and results in lower thrust force at lower pulse on-time. And as the pulse on-time increases, depth of penetration decreases, hence less number of grains pull-out at higher values of the pulse on-time. Also thermal softening is more at higher value of pulse on-time. Therefore, higher value of thrust force is recorded at higher pulse on-time. SEM photographs in Fig. 4.6(a),4.6(b),4.6(c) show heavy grain pull-out of abrasives. Loss in cutting ability is also seen in the photographs. Point analysis of Fig.4.6(b) is shown in Fig. 4.6(b1). It shows the presence of copper and cobalt in bonding material. Fig 4.6 (c) shows the cavities formed after pull-out of abrasives. Wear flat formation is also seen. Low percentage of Al (aluminium) is observed in the point analysis[Fig. 4.6(c1)] of the drill in the Fig.4.6(c). It indicates that alumina abrasive grains are pulling out from the drill. Lower thrust force is recorded for bigger grain size abrasives because pull-out of abrasive grains is more for bigger grains. Most of the abrasive grains pull-out and do not take part in machining while, in case of lower grain size, pull-out is comparatively low and comparatively more abrasives take part in machining and result in more thrust force for lower grain size.

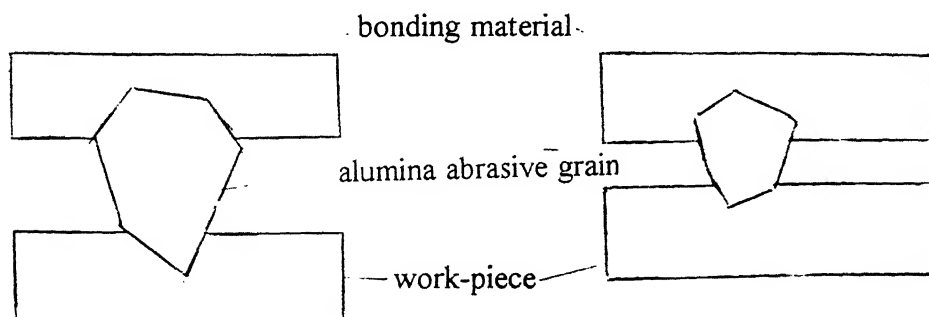
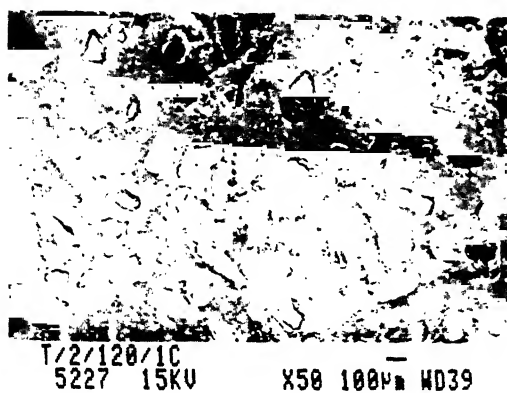
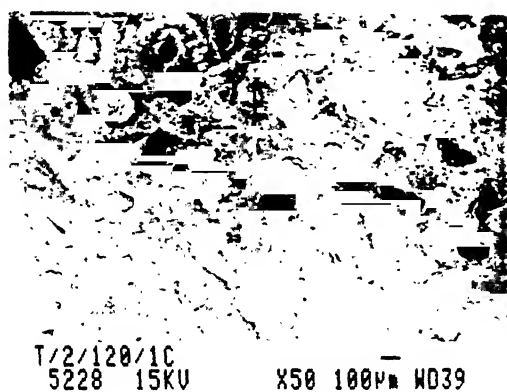


Fig. 4.5. Protrusion of grain from drill surface.



(a)



(b)



(c)

Fig.4.6 SEM photographs for drill.

# Results and Discussions

ement	Line	Weight%	K-Ratio	Cnts/s	Atomic%
	Ka	1.50	0.0156	18.61	2.01
	Ka	42.74	0.4710	223.68	46.64
	Ka	47.29	0.4663	133.27	47.87
	La	2.64	0.0227	21.93	1.43
	La	5.83	0.0436	3.63	2.04
tal		100.00			

pectrum: 031903

Range:10 keV  
Total Counts=51037. Linear Auto-VS=1326

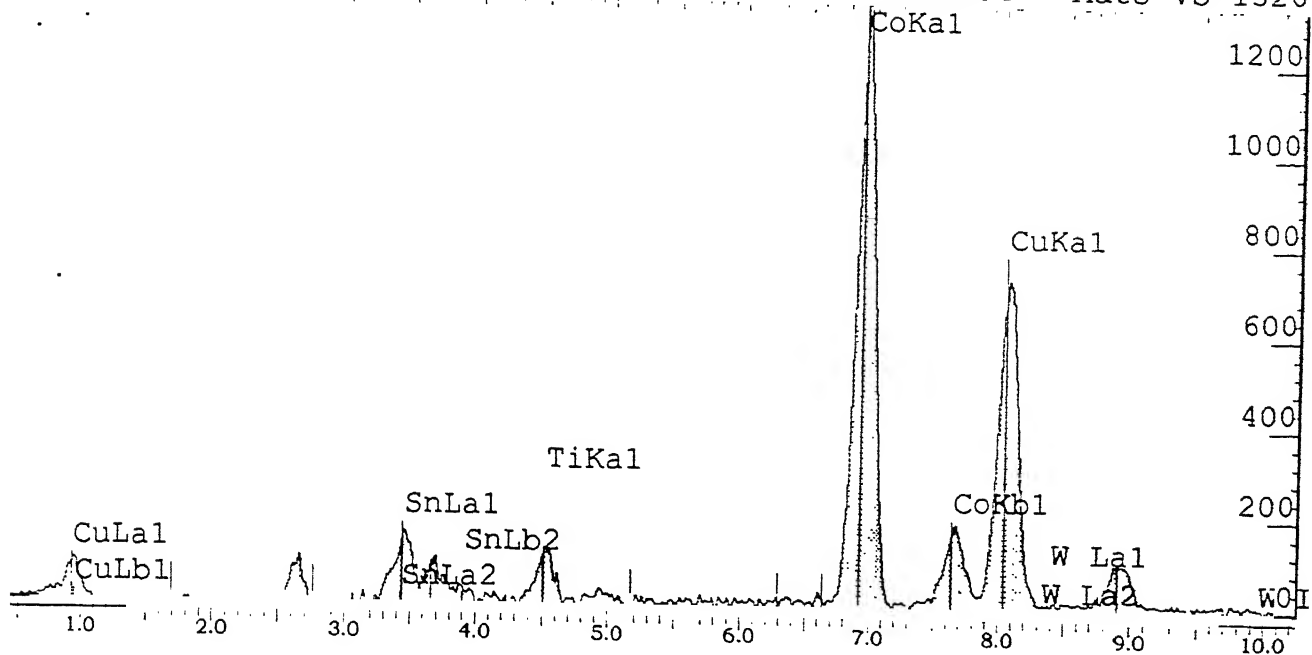


FIG. 4.6(b1)

## Results and Discussions

Element	Line	Weight%	K-Ratio	Cnts/s	Atomic%
Be	Ka	28.77	0.0442	0.17	63.46
Al	Ka	7.75	0.0608	66.93	5.71
Si	Ka	11.49	0.0962	101.39	8.13
K	Ka	28.43	0.2659	164.96	14.45
Fe	Ka	15.92	0.1380	28.70	5.67
Co	Ka	7.64	0.0647	10.82	2.58
Total		100.00			

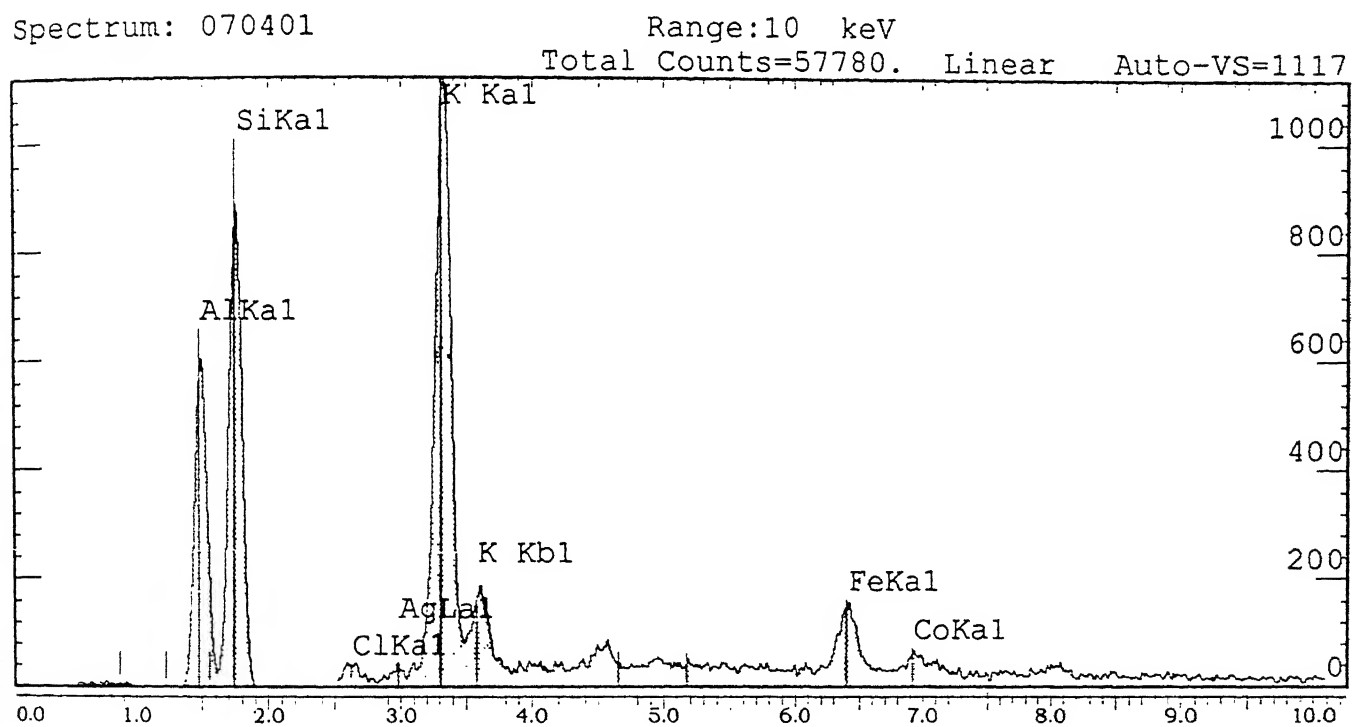


FIG. 4.6(CD)

Fig. 4.7(a) shows the trend in variation of thrust force with pulse on-time for cemented carbide work-piece. Thrust force increases with increase in pulse on-time. The reason for increase in thrust force with pulse on-time is same as stated above for Fig. 4.3. Initially, at lower pulse on-time, thrust force is low for grit size of 100/120, but it increases steeply and crosses the curve for grit size of 40/60 and at higher value of pulse on-time, thrust force is more for grit size of 100/120. Hardness of the cemented carbide is more than HSS [hardness, cemented carbide 1200-1400 Kg/mm<sup>2</sup>, HSS 750-1050 Kg/mm<sup>2</sup>]. So, at lower pulse on-time even grains of grit size 100/120 also get pulled-out from drill. Since, the area of the contact with work-piece is more for bigger grain size [Fig. 4.5], it results in more force at lower pulse on-time for grit size of 40/60. At higher pulse on-time, depth of penetration is low. Hence, grain pull-out is low for 100/120 at higher pulse on-time which results in more force at higher pulse on-time. Comparing Fig. 4.3 and Fig. 4.7(a), it is seen that thrust force is more for cemented carbide. As the hardness of the work-piece material increases, penetration of abrasives in the work-piece material reduces. As carbide possesses more hardness and wear resistance than HSS, abrasives penetrate less in cemented carbide than HSS and result in more thrust force in cemented carbide for same value of pulse on-time. Thrust force variation with pulse on-time in EDDD observed by Ankulkar[15] is shown in Fig. 4.7(b). At lower pulse on-time, thrust force in EDDD is lower than that of EDAD. But at higher value of pulse on-time, thrust force is more for EDDD. Grit blunting and pull-out is observed in EDDD[15].

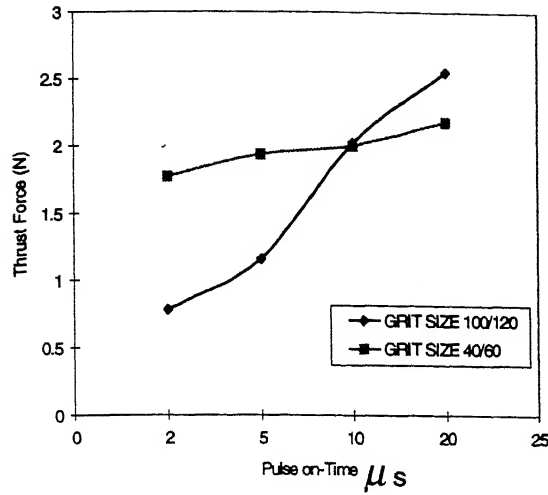


Fig.4.7(a) Thrust force variation with pulse on-time in EDAD for cemented carbide.

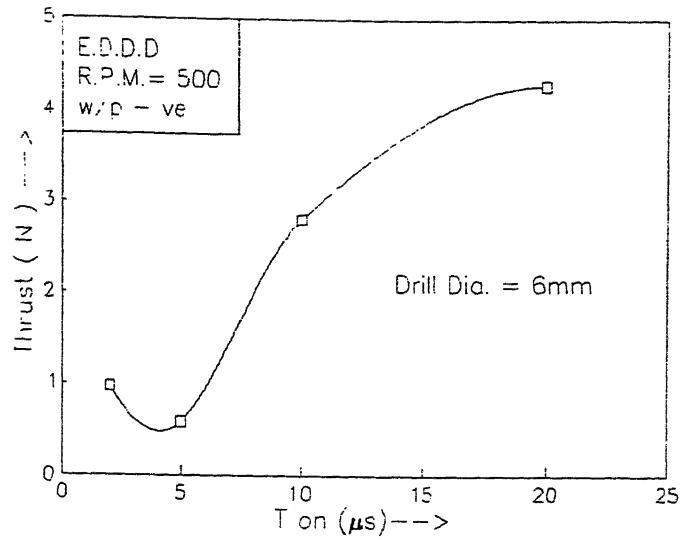


Fig. 4.7 (b) Thrust force variation with pulse on-time in EDDD for cemented carbide[15].

Almost no thrust force is observed in EDM.

## 4.2 TORQUE

Time evaluation of torque is obtained from the recorded graph. Torque values for HSS in EDAD has been plotted in Fig. 4.8. The value of torque increases with increase in pulse on-time. Torque obtained for 100/120 grit size is more than that for 40/60. This is similar to the thrust force variation. As the depth of penetration increases, thrust force increases and thus torque increases. Lower values of torque are obtained in case of HSS, since HSS possesses lower value of hardness than cemented carbide, so easier to penetrate. Fig 4.9(a) and Fig 4.9(b) show the variation of torque with pulse on-time for cemented carbide in EDAD and EDDD[reported by Ankulkar[15]] respectively. Lower value of torque is recorded for EDDD at all pulse on-time.

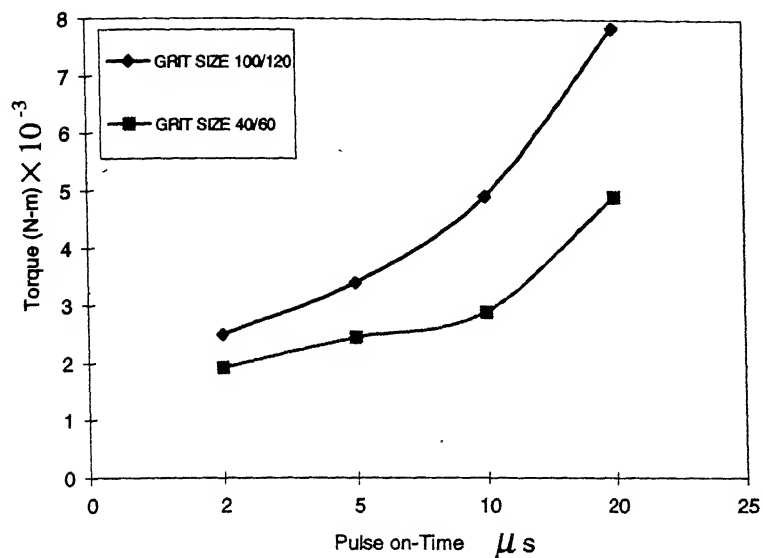


Fig. 4.8 Variation of Torque with pulse on-time in EDAD for HSS.

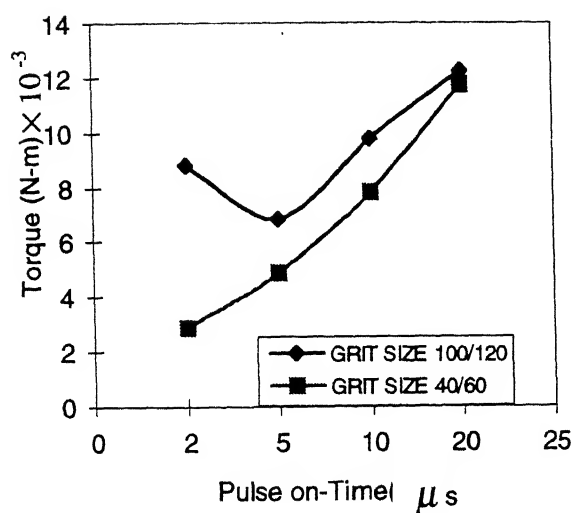


Fig.4.9(a) Variation of Torque with pulse on-time in EDAD for cemented carbide.

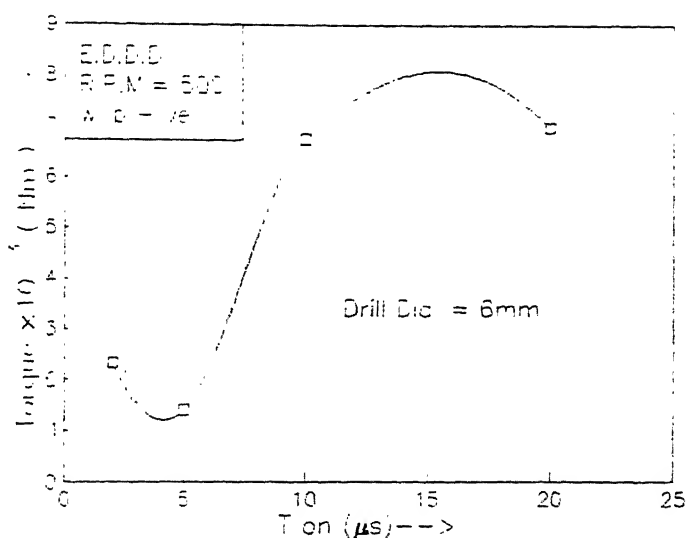


Fig.4.9(b) Variation of Torque with pulse on-time in EDDD for cemented carbide.[15]

Almost no torque is recorded in EDM, since no force is recorded.

### 4.3 PENETRATION RATE

The penetration rate has been used as a performance index here in place of MRR (material removal rate), since according to most of the researchers, MRR in drilling is assessed by penetration rate. Penetration rate has been calculated in units of mm/s. Penetration rate expresses the rate at which drill is progressing in the work-piece material. Fig. 4.10(a) shows the trend of variation of penetration rate Vs pulse on-time for cemented carbide in EDAD and Fig 4.10(b) shows the variation of penetration rate with pulse on-time for cemented carbide in EDDD reported by Ankulkar [15].

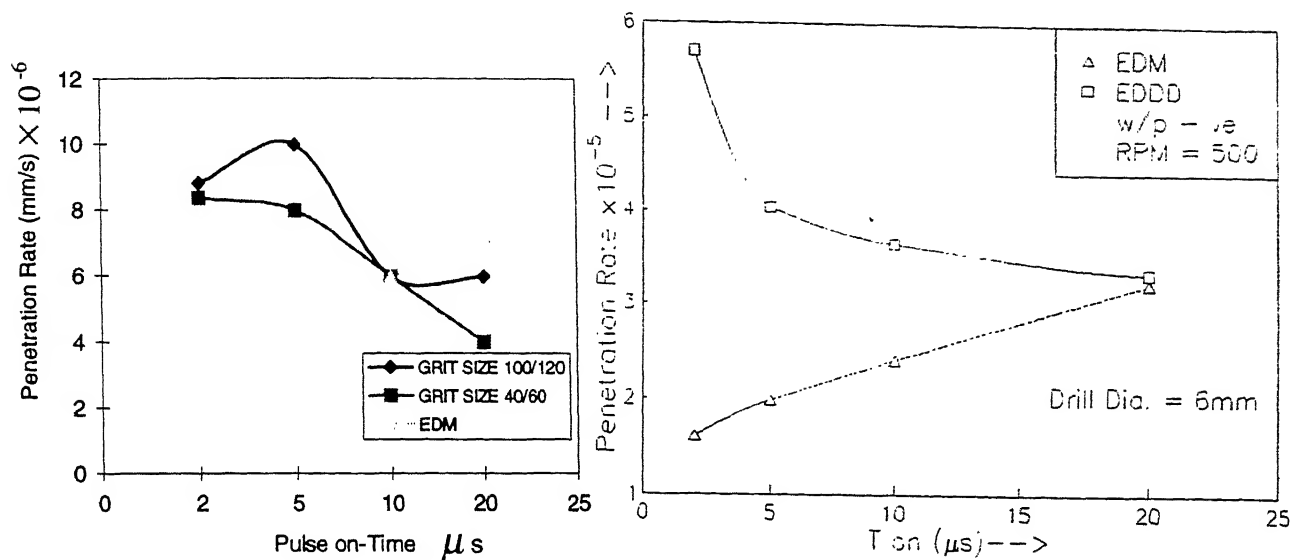


Fig.4.10(a)Variation of PR with pulse on-time in EDAD for cemented carbide. Fig.4.10(b)Variation of PR with pulse on- time in EDDD for cemented carbide[15].

For grit size of 100/120, penetration rate first increases upto 5  $\mu s$ , and after 5  $\mu s$  it decreases upto 10  $\mu s$ . And then it attains a constant value afterwards. At low pulse on-time between 2  $\mu s$  to 5  $\mu s$ , depth of penetration is more. Pull-out of abrasives is more at low pulse on-time, so grinding is less dominating at low pulse on-time and material removal is mainly due to EDM. Higher value of  $R_a$  is observed for lower pulse on-time[Refer Table 4.1]. This indicates that EDM is dominating at lower value of pulse on-time, since EDM results in poor surface finish than grinding. Material removal increases with increase in pulse on-time for EDM. The reason is that longer pulse allows more

material to melt and hence more penetration rate. Penetration rate increases from  $2\ \mu\text{s}$  to  $5\ \mu\text{s}$ . After  $5\ \mu\text{s}$  grinding starts dominating to EDM. Grinding is dominating over EDM and pull-out of abrasives is taking place so, penetration rate starts decreasing. After  $10\ \mu\text{s}$ , penetration rate curve attains a steady form, it means that a constant number of grains are continuously coming in contact with work-piece. This is only possible when the rate of pull-out of abrasive grains is equal to the rate of exposing of new grains. This can be compared with the self sharpening phenomenon in grinding. This implies that self sharpening phenomenon is taking place. This is supported by the thrust force curve (Fig. 4.3 ), which also shows approximately steady shape after  $10\ \mu\text{s}$ . Penetration rate for grit size of 40/60, is lower than the corresponding penetration rate for grit size of 100/120. It is due to two reasons.

- ~ Dominance of grinding for all pulse on-times during machining. So, the area of bonding material taking part in EDM is lower for larger grain size.
- ~ Pull-out of abrasive grains is more for grit size of 40/60 as compared to 100/120.

Since the size of these grains is bigger, and hardness of the cemented carbide is nearly equal to the abrasives [hardness, cemented carbide  $1200\text{--}1400\ \text{Kg/mm}^2$ , alumina  $1300\text{--}1400\ \text{Kg/mm}^2$ ], so abrasives can not penetrate, without thermal softening by EDM. Abrasives rub on the surface of work-piece, and they remove very less amount of material from work-piece surface. Thus, constantly decreasing curve is obtained for larger grain size drills. Penetration rate in EDDD is approximately ten times of penetration rate in EDAD. The reason is that diamond is harder than alumina and the bonding was extremely poor due to inappropriate bonding material for alumina abrasives. For both EDAD and EDDD penetration rate shows the decreasing trend with increase in pulse on-time.

Fig. 4.11 shows the variation of penetration rate with pulse on-time for HSS. A decreasing trend of penetration rate is seen upto  $10\ \mu\text{s}$ , and afterwards a steady curve is observed. HSS possesses lower value of hardness than cemented carbide, so easier to penetrate in. Lower thrust force has been observed in case of HSS. So penetration rate is more for HSS. Penetration rate is low for grit size of 40/60, reason is same as explained earlier for cemented carbide. The penetration rate curve attains a steady shape after

$10\mu s$ , which represents the self sharpening mode. Surface roughness value obtained for HSS are higher than cemented carbide. This indicates that plastic deformation mechanism is predominating in HSS. This is also supported by the SEM photographs of the chip shown in Fig. 4.25.

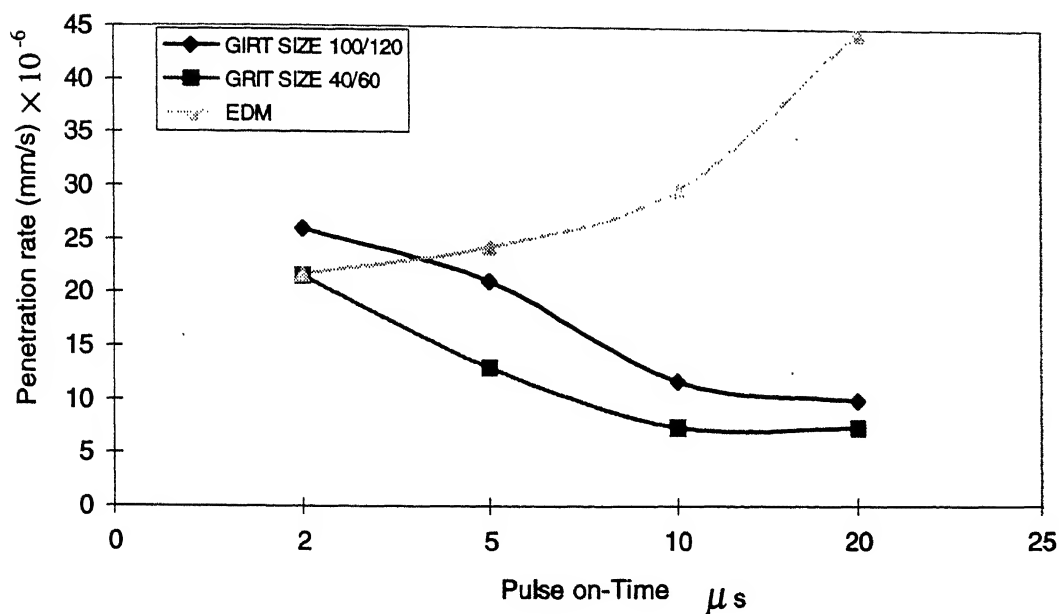
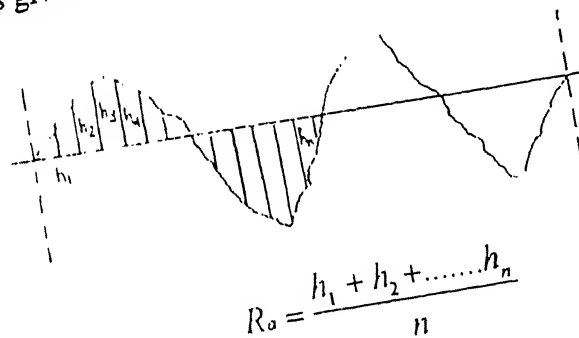


Fig. 4.11 Variation of Penetration rate with pulse on-time for HSS.

Surface roughness values obtained for cemented carbide are lower than HSS. This indicates that microcracking mechanism of fracture is predominating in cemented carbide.

## 4.4 SURFACE FINISH

Surface roughness values for unmachined and machined surfaces have been measured by Taylor Hobson Surtronic - 3P . It reads three values,  $R_a$  ,  $R_t$  and  $R_{y\max}$  . The definitions of these is given below.



$R_a$  = It is defined as the average value of the departures from its centre line throughout a prescribed sampling length.

$R_t$  = This is the maximum peak to valley height of the profile in the assessment length. [Fig. 4.12]

$R_{ti}$  = It is the maximum peak to valley height of the profile in one sampling length. [Fig. 4.12]

$R_{y\max}$  = It is the largest  $R_{ti}$  value within the assessment length.

$R_{tm}$  = It is the mean of all the  $R_{ti}$  values obtained within the assessment length.

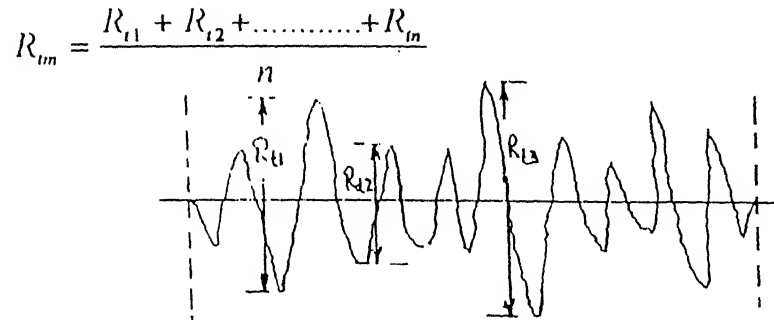


Fig.4.12 : Surface irregularities showing  $R_{ti}$  values.

Surface roughness values are given in tabular form as follows.

Table 4.1 Surface roughness values for cemented carbide.

EXP.	AFTER MACHINING						BEFORE MACHINING					
	$R_a(\mu m)$		$R_{y\max}(\mu m)$		$R_{tm}(\mu m)$		$R_a(\mu m)$		$R_{y\max}(\mu m)$		$R_{tm}(\mu m)$	
NO.		AVG.		AVG.		AVG.		AVG.		AVG.		AVG.
1 C	0.65	0.73	4.81	4.44	3.42	3.61	0.39	0.42	2.33	2.53	1.88	2.02
	0.52		4.29		3.29		0.41		2.45	2	1.97	
	0.90		3.85		4.12		0.54		3.22	2.53	2.34	
	0.86		4.79		3.62		0.35		2.12		1.90	
2 C	0.27	0.36	3.01	2.86	2.55	2.19	0.49	0.60	3.14	3.50	2.42	2.7
	0.38		2.64		1.97		0.66		3.55		2.84	
	0.43		2.90		2.15		0.56		3.51		2.61	
	0.36		2.87		2.08		0.67		3.80		2.93	
3 C	0.34	0.38	3.91	3.23	2.26	2.57	0.39	0.42	2.33	2.53	1.88	2.02
	0.41		2.38		2.32		0.41		2.45		1.97	
	0.45		3.28		2.78		0.54		3.22		2.34	
	0.31		3.34		2.91		0.35		2.12		1.90	
4 C	0.65	0.74	4.35	5.15	3.78	3.95	0.61	0.84	4.85	5.70	3.74	4.44
	0.78		6.79		4.53		1.02		6.56		5.40	
	0.54		3.40		2.99		0.78		5.43		4.01	
	0.98		6.07		4.50		0.94		5.96		4.60	

5 C	0.60	0.67	4.01	4.48	2.81	3.16	0.59	0.58	5.31	4.69	3.10	2.69
	0.70		5.01		3.17		0.64		4.72		2.66	
	0.63		3.94		2.94		0.51		4.14		2.32	
	0.74		4.97		3.70		0.56		4.62		2.68	
6 C	0.65	0.48	4.56	3.53	2.69	2.68	0.88	0.68	4.93	5.02	5.10	3.59
	0.52		2.96		2.45		0.70		8.61		3.38	
	0.43		3.72		2.87		0.47		2.90		2.60	
	0.30		2.89		2.72		0.68		3.62		3.26	
7 C	0.35	0.54	3.83	4.13	2.89	3.24	0.32	0.39	2.83	3.10	1.52	1.83
	0.55		3.64		3.65		0.39		2.44		1.80	
	0.60		3.82		3.17		0.45		4.01		2.09	
	0.65		5.22		3.23		0.41		3.11		1.92	
8 C	0.81	0.69	5.89	4.93	3.64	3.41	.97	0.63	5.44	2.93	2.80	1.93
	0.45		2.86		2.36		.39		1.82		1.69	
	0.99		7.51		4.61		.37		1.81		1.40	
	0.53		3.47		3.01		.78		2.63		1.84	
1CE	0.54	0.48	2.89	2.91	2.35	2.16	0.59	0.58	5.31	4.69	3.10	2.69
	0.43		2.61		2.27		0.64		4.72		2.66	
	0.50		3.41		1.98		0.51		4.14		2.32	
	0.45		2.72		2.04		0.56		4.62		2.68	
2CE	0.25	0.44	3.16	2.98	2.18	2.5	0.88	0.68	4.93	5.02	5.10	3.59
	0.50		2.82		2.55		0.70		8.61		3.38	
	0.38		2.58		2.26		0.47		2.90		2.60	
	0.61		3.34		3.01		0.68		3.62		3.26	
3CE	0.57	0.56	4.83	4.22	3.67	3.62	0.32	0.39	2.83	3.10	1.52	1.83
	0.42		3.81		3.27		0.39		2.44		1.80	
	0.56		3.92		3.30		0.45		4.01		2.09	
	0.69		4.30		4.25		0.41		3.11		1.92	
4CE	0.76	0.85	6.02	6.04	4.99	4.52	0.97	0.63	5.44	2.93	2.80	1.93
	1.04		6.62		3.59		0.39		1.82		1.69	
	0.76		5.61		5.20		0.37		1.81		1.40	
	0.84		5.89		4.28		0.78		2.63		1.84	

Table 4.2 Surface roughness values for HSS.

EXP NO.	AFTER MACHINING						BEFORE MACHINING					
	$R_a$ ( $\mu m$ )		$R_{ymax}$ ( $\mu m$ )		$R_{tm}$ ( $\mu m$ )		$R_a$ ( $\mu m$ )		$R_{ymax}$ ( $\mu m$ )		$R_{tm}$ ( $\mu m$ )	
		AVG.		AVG.		AVG.		AVG.		AVG.		AVG.
1H	1.73	1.31	16.01	10.14	8.44	7.67	0.87	0.78	9.55	8.18	3.67	3.00
	1.22		9.20		7.63		0.99		8.67		3.03	
	1.15		7.32		8.04		0.45		6.34		2.43	
	1.13		8.04		6.57		0.79		8.14		2.88	
2H	0.90	0.82	5.64	5.70	4.16	3.99	0.34	0.64	2.95	6.43	1.44	1.79
	0.78		6.10		3.92		1.23		13.66		1.89	
	0.78		6.35		4.24		0.34		3.93		2.04	
	0.82		4.72		3.66		0.63		5.17		1.78	
3H	1.68	1.79	11.61	13.17	10.22	10.10	0.21	0.23	1.13	1.05	0.84	0.84
	2.02		17.71		10.85		0.17		0.89		0.73	
	1.79		14.03		10.74		0.30		1.12		0.99	
	1.65		9.33		8.59		0.23		1.05		0.78	
4H	1.26	1.37	11.79	10.27	7.65	7.65	0.73	0.69	5.73	7.00	3.45	2.56
	1.31		10.16		7.98		0.42		3.17		2.37	
	1.62		9.68		7.50		1.01		10.36		1.98	
	1.29		9.43		7.48		0.59		8.73		2.43	
5H	2.16	2.37	15.51	16.06	13.17	13.75	0.33	0.46	3.88	4.89	2.60	3.07
	2.37		16.11		13.99		0.53		5.80		3.56	
	2.36		15.01		13.37		0.43		4.57		2.89	
	2.57		17.67		14.47		0.56		5.33		3.24	
6H	3.40	2.72	27.80	23.29	15.39	13.89	1.11	0.74	10.87	2.55	4.12	2.3
	2.00		17.04		9.96		0.17		2.98		1.46	
	2.62		24.14		12.64		0.69		1.78		1.78	
	2.85		24.18		17.55		0.98		3.57		1.84	
7H	1.02	1.23	8.12	9.93	5.39	7.23	0.15	0.33	1.09	4.28	1.15	1.32
	1.23		10.84		6.91		0.58		11.29		1.52	
	1.39		9.81		8.55		0.26		1.93		1.36	
	1.29		10.93		8.08		0.33		2.79		1.23	

8H	2.14	2.62	20.23	19.49	13.77	13.69	0.19	0.21	1.93	1.52	1.49	1.23
	2.25		16.58		11.62		0.17		1.34		1.10	
	3.12		22.41		15.82		0.26		1.46		1.18	
	2.95		18.77		13.58		0.21		1.34		1.13	
1HE	3.23	3.22	22.89	23.56	18.34	17.55	0.33	0.46	3.88	4.89	2.60	3.07
	3.46		24.76		17.32		0.53		5.80		3.56	
	3.03		23.40		15.41		0.43		4.57		2.89	
	3.17		23.19		19.12		0.56		5.33		3.24	
2HE	3.09	3.35	21.32	23.06	17.50	17.86	1.11	0.74	10.87	2.55	4.12	2.3
	3.77		25.48		20.87		0.17		2.98		1.46	
	3.10		19.51		15.30		0.69		1.78		1.78	
	3.44		25.92		17.77		0.98		3.57		1.84	
3HE	2.43	2.44	15.36	17.02	12.54	13.08	0.15	0.33	1.09	4.28	1.15	1.32
	2.60		19.23		14.45		0.58		11.29		1.52	
	2.63		19.87		13.81		0.26		1.93		1.36	
	2.10		13.62		11.50		0.33		2.79		1.23	
4HE	1.50	1.44	9.47	8.93	8.52	8.41	0.19	0.21	1.93	1.52	1.49	1.23
	1.49		8.60		8.36		0.17		1.34		1.10	
	1.33		9.32		8.43		0.26		1.46		1.18	
	1.44		8.34		8.33		0.21		1.34		1.13	

Table 4.3 Change in surface roughness value.(  $\Delta R_a$  = Final  $R_a$  - Initial  $R_a$  )

EXP.NO.	$\Delta R_a(\text{AVG.})(\mu\text{m})$	EXP.NO.	$\Delta R_a(\text{AVG.})(\mu\text{m})$
1 C	0.31	1 H	0.53
2 C	-0.24	2 H	0.18
3 C	-0.04	3 H	1.56
4 C	-0.1	4 H	0.68
5 C	0.9	5 H	1.91
6 C	-0.2	6 H	1.98
7 C	0.15	7 H	0.9
8 C	-0.6	8 H	2.41
1 CE	-0.1	1 HE	2.76

2 C E	-0.24	2 H E	2.61
3 C E	0.17	3 H E	2.11
4 C E	0.22	4 H E	1.23

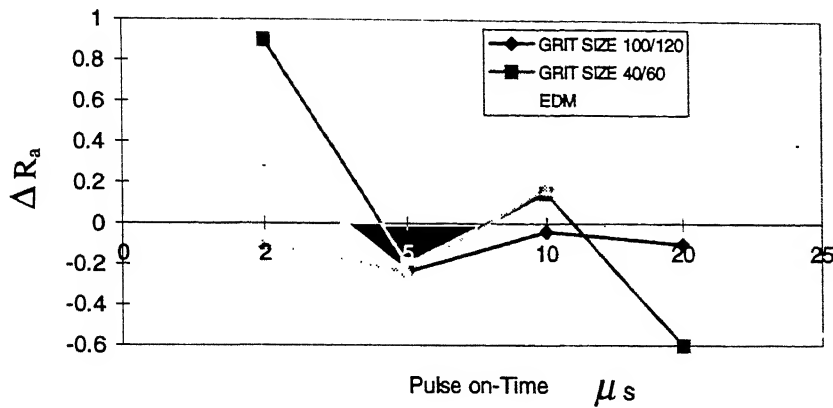


Fig 4.13 Change in surface roughness (  $\Delta R_a$  ) for cemented carbide.

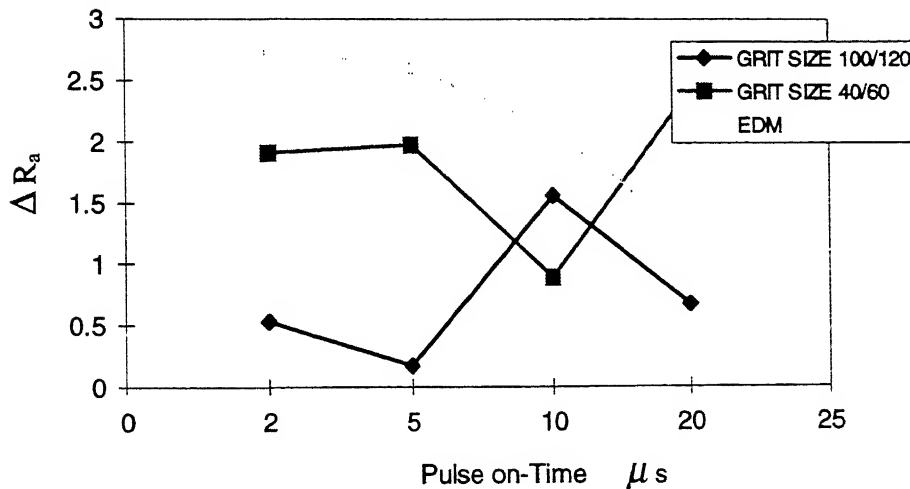
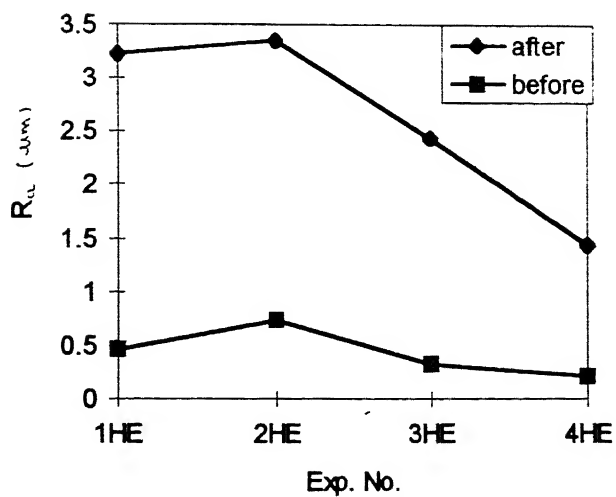
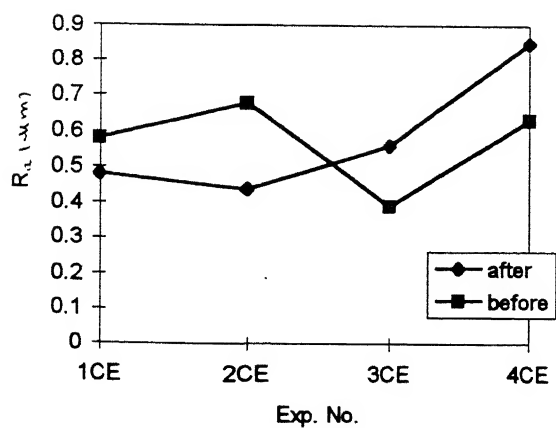
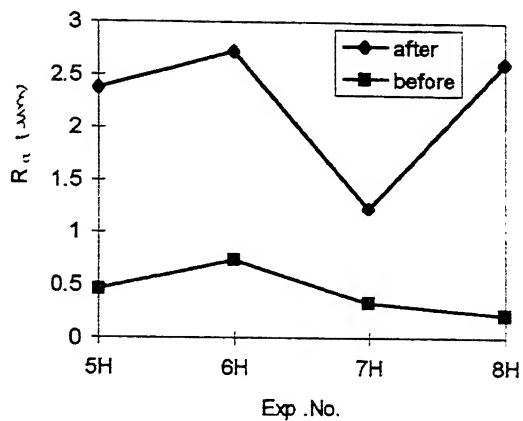
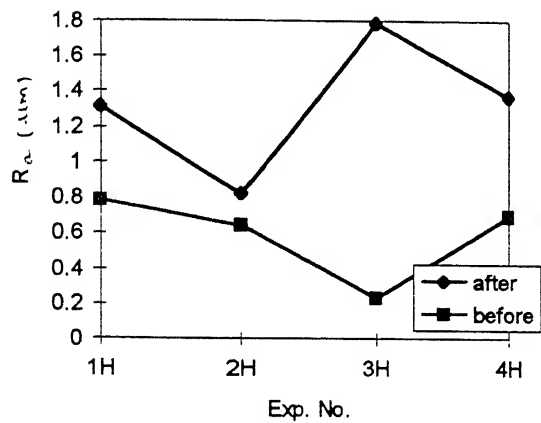
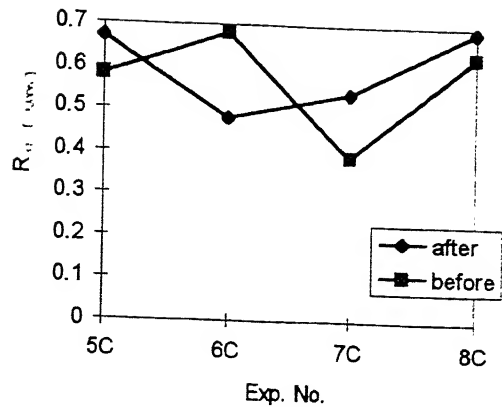
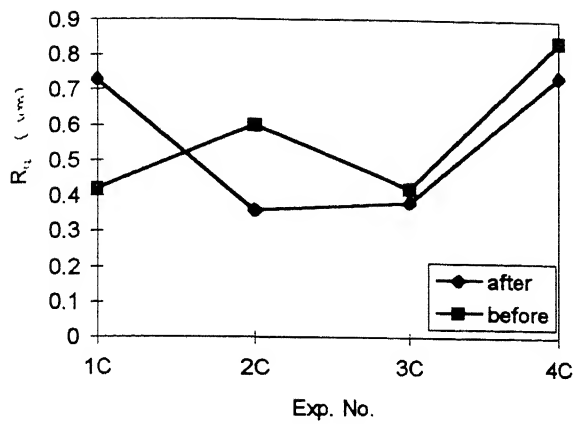


Fig. 4.14 Change in surface roughness (  $\Delta R_a$  ) for HSS.

Surface roughness values ( $R_a$ ) are plotted in Fig 4.15 for all the experiments. Change in  $R_a$  ( $\Delta R_a$ ) is also plotted in Fig. 4.13 and Fig. 4.14. It is clear that surface roughness values for cemented carbide are less than that of HSS because microcracking mechanism of material removal is dominating in cemented carbide. In all the experiments poor surface finish is obtained after machining. This is evident from the SEM photograph in Fig. 4.16.



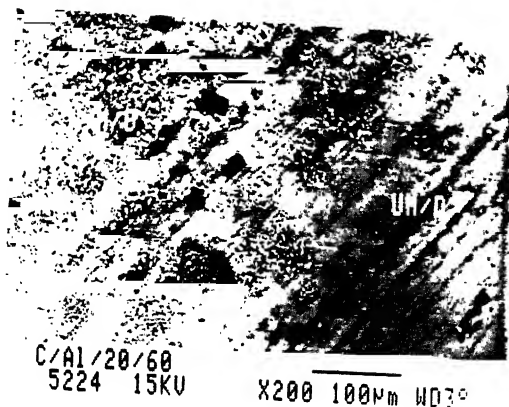
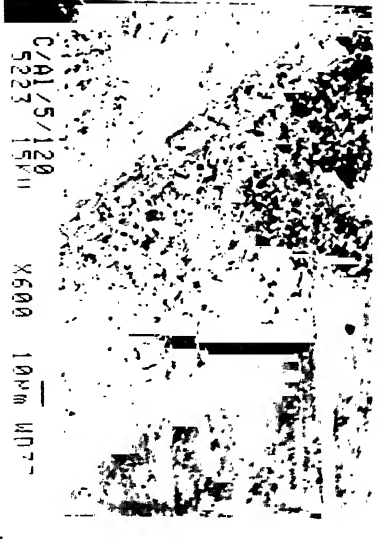

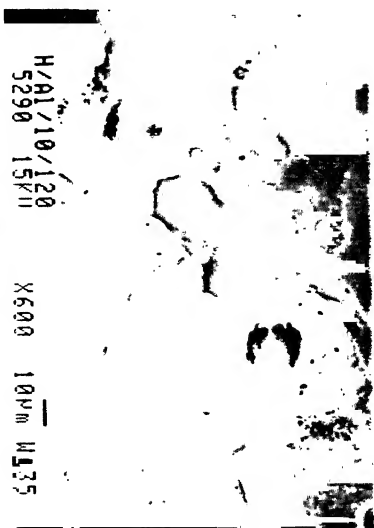






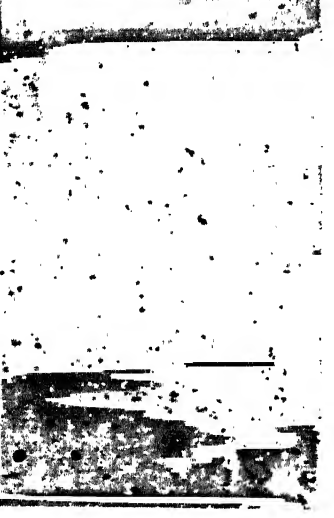
Fig. 4.16

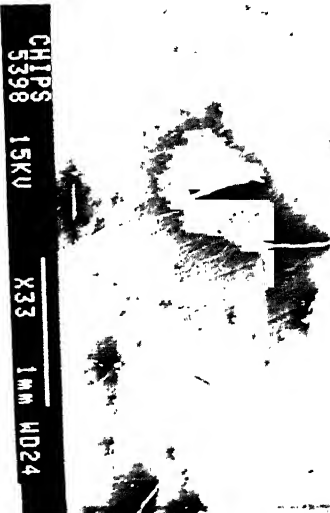
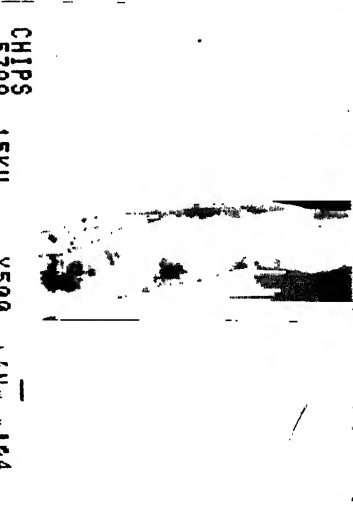
## 4.5 SEM ANALYSIS

SEM analysis has been done by scanning electron microscope and photographs have also been taken to explain the process. Fig.4.17 shows the machined and unmachined surface, grinding marks are visible. Craters are formed at the outer periphery of the drill. Bulk analysis [Fig. 4.27] of the surface shown in Fig 4.17 shows the presence of Ti(Titanium). Fig 4.18 shows the recast layer because of cohesion poorer surface finish is observed after EDAD. Point analysis[Fig 4.46] of the surface shows the presence of aluminium. Fig 4.19 shows the alumina grain embedded in the work-piece surface. Fig.4.20 shows the chips formed during EDAD. Pulled out abrasive grain is also visible in Fig 4.20. Fig. 4.21 shows the work surface machined by EDM. Recast layer is also visible. In Fig.4.22, pulled out grains and chips are visible. In Fig. 4.23, a globule formed during EDAD of HSS is seen. The enlarged view of the surface of this globule is shown in Fig.4.24. Chips have been collected by filtering the electrolyte and photographs of these chips are seen in the Fig 4.25 and Fig 4.26. Fig 4.26 shows the magnified view of the chip, burrs on the chip are clearly visible.

<p>1.</p> 	<p>Fig. 4.17</p> <ol style="list-style-type: none"> <li>1. Grinding marks are seen.</li> <li>2. Craters are formed at outer periphery of drill.</li> <li>3. Bulk analysis shows the presence of Ti.</li> </ol>	<p>Experiment No. 2C  <math>T_{ON} = 5 \mu s</math>,  Grit size 100/120  W/P CC</p>
<p>2.</p> 	<p>Fig. 4.18</p> <ol style="list-style-type: none"> <li>1. Heavy grain pull-out</li> <li>2. Loss in cutting ability</li> <li>3. EDM effect on bonding material is seen (craters are formed).</li> <li>4. Point analysis shows presence of copper in bonding material.</li> </ol>	<p>Experiment No. 1C  <math>T_{ON} = 2 \mu s</math>,  Grit size 100/120  Tool</p>

3.	 <p>H/A1/10/120 5290 15KV X600 100µm W135</p>	Fig.4.19	<p>1. Alumina grain embedded in w/p is seen. 2. Recast layer is formed.</p>	<p>Experiment No. 3H T<sub>ON</sub> = 10 µs, Grit size 100/120 w/P HSS</p>
4.	 <p>H/A1/5/60 5369 15KV X700 100µm W135</p>	Fig.4.20	<p>1. Chips are seen on the work surface. 2. Pulled out abrasive grain is also seen.</p>	<p>Experiment No. 6H T<sub>ON</sub> = 5 µs, Grit size 40/60 w/P HSS</p>
5.	 <p>EDM/4HE 5371 15KV X300 100µm W035</p>	Fig. 4.21	<p>1. Large number of craters. 2. Recast layer is formed.</p>	<p>Experiment No. 4HE T<sub>ON</sub> = 20 µs, w/P HSS EDM</p>

6.		<p>1. Pulled out abrasive grains are seen.</p> <p>2. Chips are also seen.</p>	<p>Experiment No. 8H</p> <p><math>T_{ON} = 20 \mu s</math>,</p> <p>Grit size 40/60</p> <p>W/P HSS</p>
7.		<p>1. Globule is seen.</p>	<p>Experiment No. 8H</p> <p><math>T_{ON} = 20 \mu s</math>,</p> <p>Grit size 40/60</p> <p>W/P HSS</p>
8.		<p>1. On the surface of the globule, craters are seen.</p> <p>2. Small size of craters.</p> <p>3. Less number of craters.</p>	<p>Experiment No. 8H</p> <p><math>T_{ON} = 20 \mu s</math>,</p> <p>Grit size 40/60</p> <p>W/P HSS</p>

9.		Fig. 4.25	1. Plastically deformed chips are seen.	Experiment No. 8H $T_{ON} = 20 \mu s$ , Grit size 40/60 w/P HSS
10.		Fig. 4.26	1. Burrs on the chip are seen.	Experiment No. 8H $T_{ON} = 20 \mu s$ , Grit size 40/60 w/P HSS

Element	Line	Weight%	K-Ratio	Cnts/s	Atomic%
Al	Ka	0.12	0.0009	1.35	0.30
Si	Ka	0.41	0.0045	3.48	0.68
Ti	Ka	35.22	0.3638	215.07	48.60
Co	Ka	13.81	0.1468	34.61	15.49
Ni	Ka	9.82	0.1082	20.06	11.05
Cu	Ka	13.61	0.1397	19.82	14.16
W	La	27.00	0.2077	8.59	9.71
Total		99.99			

Spectrum: 031901

Range: 10 keV  
Total Counts=42848. Linear Auto-VS=1375

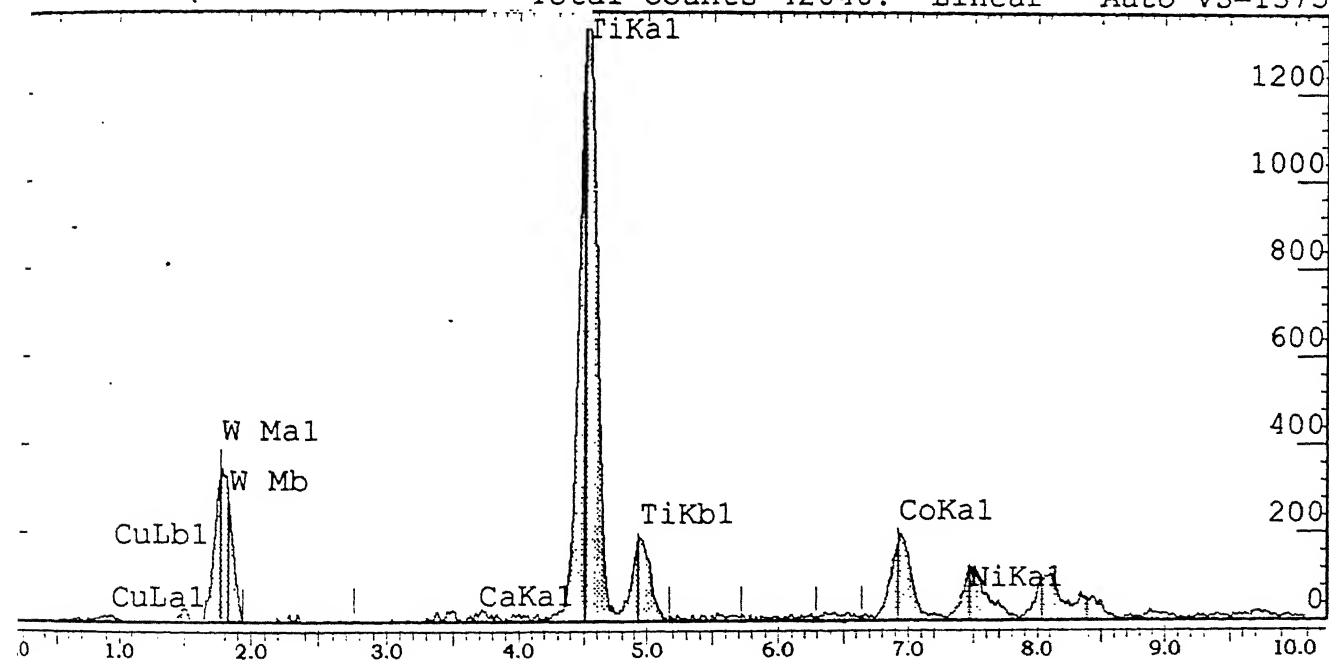


Fig.4.27

CENTRAL LIBRARY  
No. A 125485

# **CHAPTER FIVE**

## **CONCLUSIONS**

Following conclusions have been derived from the EDAD experiments done on cemented carbide and HSS.

1. SEM photographs and results have shown heavy abrasive grain pull-out in all the EDAD experiments. Since the bonding material used for manufacturing of these EDAD drilling points is copper berrillium which does not provide good wettability with alumina hence provides poor bonding strength.
2. Low penetration rate is observed for bigger grain size. Since bonding strength of copper berrillium is not good, grains pull-out without cutting occurs. The probability of pull-out in bigger grains is more. Low thrust force and torque values are obtained for bigger grain size.
3. Penetration rate for HSS is more than that of cemented carbide. HSS (hardness 750 -1050 Kg/mm<sup>2</sup>) has less hardness than cemented carbide (1200-1400 Kg/mm<sup>2</sup>). Hardness of abrasive alumina grains is nearly equal to cemented carbide, so material removal in case of HSS is more.
4. Thrust force and torque values obtained are more for cemented carbide, as it is comparatively difficult to indent.
5. Penetration rate curve attains a steady value after 10  $\mu$  s for 100/120 grit size. This is possible only when the rate of pull-out of abrasives is equal to the rate of exposing of fresh abrasive grains. This can be compared with self sharpening phenomena.

6. Penetration rates obtained for HSS and cemented carbide both are lower than that of EDM. Since most of the grains pull-out and do not participate in cutting effectively, EDM dominates to grinding. The area of abrasive tool taking part in EDM is low in case of EDAD which results in low penetration rate for EDAD.

# **CHAPTER SIX**

## **SCOPE FOR FUTURE WORK**

1. Some other bonding materials which are having bonding strength better than copper berrillium can be used for bonding alumina abrasive grains in metal bonded points.
2. Metal bonded points of abrasives having hardness in between alumina and diamond can be tried for EDAD.
3. Surface fininsh obtained is bad in case of EDAD. So abrasives of smaller grain size may be used to improve surface fininsh. Pull-out of abrasives is more in bigger grain size that can also be avoided.

## REFERENCES

1. Larsen-Basse and N. Devnani, 'Binder extrusion as a controlling mechanism in abrasion of WC-Co cemented carbides', *Proc. Int. Conf. Science of Hard Materials*, Eds. 2. E. A. Almond, C. A. Brookes and R. Warren, Adam Hilger Ltd., Bristol, pp-883-895, (1986).
2. Rubenstein, 'The mechanics of grinding', *Int. J. Mach. Tool Des. Res. Vol. 12 pp. 127 - 139*.
3. Zelwar and S. Malkin, 'Grinding of WC-Co cemented carbides', *J. Eng. Ind.*, pp-209-220, 102 (1980).
4. Ritter and S. Malkin, 'Grinding Mechanisms and Strength Degradation for Ceramics' *Journal of Engineering for Industry May 1989, Vol. 111 pp. 167 - 173*.
5. Larsen-Basse, 'Abrasive wear of tungsten carbide - cobalt composites. I. Rotary drilling tests' *Materials Science and Engineering*, 13(1974) 83 - 91
6. Moore, and F. S. King, 'Abrasive wear of brittle solids', *WEAR*, pp 123 -140, 60 (1980).
7. Pandey & S. T. Jilani, 'Electrical machining characteristics of cemented carbides', *WEAR*, pp 77 - 88, 116 (1987).
8. A.M.Gadalla and W. Tsai, 'Electrical discharge machining of tungsten-carbide cobalt composites', *J. Am. Ceram. Soc.*, pp-1396-1401, 72 [8] (1989).
9. Lenz, E. Katz, W. Konig, TH Aachen, and W. Gemany, 'Cracking behaviour of sintered carbides during EDM'.
10. Philip Koshy, V. K. Jain, and G. K. Lal, 'Mechanism of material removal in electrical discharge diamond grinding', *Int. Journal of Mac. Tool and Mamufacture*, pp 1173-1185, 36 (1996).
11. Uematsu, K.Suzuki, T. Yanase and T. Nakagawa, 'A new complex grinding method for ceramic materials combined with ultrasonic vibration and electrodischarge machining', *Intersociety Symposium on Machining of Ceramic Materials*, Eds. S. Chandrasekhar et al., American Society of Mechanical Engineers, New York, 135 - 140 (1988).

12. Kitagawa and K. Maekawa , 'Plasma hot machining for new engineering materials' *Wear* 139 (1990) 251 - 267.
13. Copper G.A. , 'Some observations on environmental effects when diamond drilling', The science of ceramic machining and surface finishing II, B.J. Hockey and R.W. Rice, eds, *National Bureau of Standards Special Publication 562*, U.S. Government printing office, Washington, D.C. pp 115 - 138 (1979).
14. E.Ya Grodzinskii and L.S. Zubotava, 'Electrochemical and electrical-discharge abrasive machining', *Sov. Eng.Res.* 2 (3), 90 - 92 (1982).
15. Ankulkar M.S., 'Electric discharge diamond drilling of cemented carbides.' Masters Thesis. August 1997, I I T Kanpur.
16. Ogilvy, 'On the indentation fracture of cemented carbide - Survey of operative fracture modes' ,*Wear* ,43 (1977) 239-252.
17. Blombery R.I., Perrot C.M., Robinson P.M. , 'Abrasive wear of tungsten carbide-cobalt composites. I. wear mechanisms' , *Materials Science and Engineering*, 13 (1974) 93-100.
18. Metzger J.L., Torrance A., 'Dry versus wet grinding of cemented carbide, *Industrial Diamond Review*, No. 6, (1990) pp. 296-303.
19. Graham W., Nee A., 'The grinding of tool steels with a diamond abrasive wheel' , *Int. J. Mach. Tool Des. Res.* Vol. 14, pp. 175-185
20. Philip Koshy, V. K.Jain and G.K. Lal, 'Grinding of cemented carbide with electrical spark assist', *J. Mat. Pro. Tech.*, To be published.

# APPENDIX 1

<u>WRKPIECE MATERIAL</u>	<u>COMPOSITION</u>	<u>PARTICLE SIZE</u>
		$\mu\text{m}$ )
1. CEMENTED	(a) WC - 20.0 %	1.0 - 1.5
CARBIDE	(b) TiC + TiN + TaC - 61.0 %	1.0 - 2.0
	(c) Ni + Co + Mo - 19.0 %	1.0 - 2.0
SINTERED PROPERTIES	(a) Density - 7.1 gm / cm <sup>3</sup> .	
	(b) Thermal conditions - 20 W m <sup>-1</sup> K <sup>-1</sup> .	
	(c) TRS - 2500 N / mm <sup>2</sup> .	
SINTERED CONDITIONS	(a) Sintering Temperature - 1480 °C.	
	(b) Holding Time - 60 minutes.	
	(c) Sintering Atmosphere - Vacuum.	
2. HSS (High Speed Steel)	(a) Fe - 76.25 %	
	(b) W - 18 %	
	(c) Cr - 4 %	
	(d) V - 1 %	
	(c) C - 0.75 %	
SINTERED PROPERTIES	(a) Density - 7.85 gm/cm <sup>3</sup> .	

## APPENDIX 2

Table 2 (A) Results of EDAD for cemented carbide work-piece.

EXP. NO.	THRUST FORCE (N)	TORQUE (N-m) $\times 10^{-3}$	PENETRATION RATE (mm/sec) $\times 10^{-6}$	GRIT SIZE	WORK-PIECE MATERIAL
1 C	0.78	8.83	8.79	100/120	cemented carbide
2 C	1.16	6.87	9.96	100/120	cemented carbide
3 C	2.02	9.81	5.98	100/120	cemented carbide
4 C	2.55	12.26	5.98	100/120	cemented carbide
5 C	1.77	2.9	8.37	40/60	cemented carbide
6 C	1.94	4.9	7.97	40/60	cemented carbide
7 C	2.00	7.85	5.97	40/60	cemented carbide
8 C	2.18	11.77	3.99	40/60	cemented carbide

Table 2 (B) Results of EDAD for HSS work-piece.

EXP. NO.	THRUST FORCE (N)	TORQUE (N-m) $\times 10^{-3}$	PENETRATION RATE (mm/sec) $\times 10^{-6}$	GRIT SIZE	WORK-PIECE MATERIAL
1 H	0.38	2.50	26.00	100/120	HSS
2 H	0.51	3.40	21.00	100/120	HSS
3 H	0.61	4.90	11.70	100/120	HSS
4 H	0.67	7.85	10.00	100/120	HSS
5 H	0.26	1.93	21.60	40/60	HSS
6 H	0.31	2.45	13.00	40/60	HSS
7 H	0.43	2.90	7.46	40/60	HSS
8 H	0.57	4.90	7.43	40/60	HSS

Table 2 (C) Results of EDM for HSS work-piece.

EXP. NO.	THRUST FORCE (N)	TORQUE (N-m) $\times 10^{-3}$	PENETRATION RATE (mm/sec) $\times 10^{-6}$	WORK-PIECE MATERIAL
1 HE	0.0	0.0	21.62	HSS
2 HE	0.0	0.0	24.33	HSS
3 HE	0.0	0.0	29.7	HSS
4 HE	0.0	0.0	44.6	HSS

Table 2 (D) Results of EDM for cemented carbide work-piece.

EXP. NO.	THRUST FORCE (N)	TORQUE (N-m) $\times 10^{-3}$	PENETRATION RATE (mm/sec) $\times 10^{-6}$	WORK-PIECE MATERIAL
1 CE	0.0	0.0	3.58	cemented carbide
2 CE	0.0	0.0	4.66	cemented carbide

289021

3 CE	0.0	0.0	5.97	cemented carbide
4 CE	0.0	0.0	7.17	cemented carbide